**NASA Contractor Report** 182087

# COMPARISON OF DIGITAL CONTROLLERS USED IN MAGNETIC SUSPENSION AND BALANCE SYSTEMS

William A. Kilgore

OLD DOMINION UNIVERSITY
RESEARCH FOUNDATION
Norfolk, Virginia

Grant NAG1-1056
December 1990

National Aeronautics and
Space Administration

**Langley Research Center**
Hampton, Virginia 23665-5225

## SUMMARY

Dynamic systems that were once controlled by analog circuits are now controlled by digital computers. Presented is a comparison of the digital controllers presently used with magnetic suspension and balance systems. The overall responses of the systems are compared using a computer simulation of the magnetic suspension and balance system and the digital controllers. The comparisons include responses to both simulated force and position inputs. A preferred digital controller is determined from the simulated responses.

ACKNOWLEDGEMENTS

I wish to thank the many people who have helped in this research. Foremost is my graduate advisor, Dr Colin P. Britcher, for his help, guidance and patience. Further appreciation must go to Dr. S. Balakrishna for providing an understanding and guidance during this research.

This work was partly supported by NASA Grants NAG-1-716 and NAG-1-1056.

TABLE OF CONTENTS

Page

SUMMARY ..... i

ACKNOWLEDGEMENTS ..... ii

TABLE OF CONTENTS ..... iii

LIST OF SYMBOLS ..... v

NOMENCLATURE ..... vii

LIST OF TABLES ..... viii

LIST OF FIGURES ..... ix

Chapter

1. INTRODUCTION ..... 1

2. GOVERNING EQUATIONS ..... 4

   2.1 Dynamics of the Suspended Body ..... 6

   2.2 Governing Equation of the Magnetic Coil ..... 8

   2.3 Single Degree-of-Freedom MSBS Transfer Function ..... 10

   2.4 State-Space Representation ..... 14

3. MAGNETIC SUSPENSION AND BALANCE SYSTEM CONTROLLERS ..... 16

   3.1 Phase-Advance Controller ..... 17

   3.2 Proportional-Integral-Derivative Controller ..... 19

4. CONTROLLERS ..... 20

   4.1 Development of Digital Controllers for Wind Tunnel MSBSs ..... 20

      4.1.1 Oxford, England ..... 20

      4.1.2 MIT, United States ..... 21

      4.1.3 Southampton, England ..... 22

      4.1.4 NASA Langley, United States ..... 25

      4.1.5 NAL, Japan ..... 26

4.2 Other Digitally Controlled Magnetic Suspension Systems ....27
4.2.1 Loughborough, England ....27
4.2.2 Mitsui Engineering and Shipbuilding, Japan ....30
4.2.3 Oak Ridge Gaseous Diffusion Plant, United States ....33
4.2.4 UVa Electrical Engineering, United States ....36
4.2.5 UVa Nuclear Engineering and Engineering Physics, United States ....37
5. DIGITAL SIMULATION ....39
5.1 Derivation of Equations for Simulation ....39
5.2 Simulation Program ....40
5.3 Representative Magnetic Suspension and Balance System ....41
6. COMPARISON OF CONTROLLERS BY SIMULATION PROGRAM ....43
6.1 Location of Controller ....43
6.2 Comparison of Dual Phase-Advance Controllers ....48
6.2.1 5% Overshoot Performance ....49
6.2.2 Minimum First Overshoot Performance ....52
6.2.3 Execution Times ....54
6.3 Comparison of Proportional-Integral-Derivative Controllers ....55
6.3.1 Minimum First Overshoot Performance ....56
6.3.2 Execution Times ....59
7. CONCLUSIONS AND RECOMMENDATIONS ....60
7.1 Best Overall Controller ....60
7.2 Future Methods of Control ....61
7.3 Effects that any Approximations may have on Results ....62
7.4 Applications to Multi-Degree-of-Freedom Systems ....63
REFERENCES ....64
APPENDICES
A. Program Listing ....67
B. Tustin's Method of Transformation ....80

## LIST OF SYMBOLS

| | |
|---|---|
| A | numerator variable in phase-advance controller |
| a, b | constant with integer subscripts |
| B | denominator variable in phase-advance controller |
| C | damping coefficient |
| $\frac{d}{dt}$ | derivative with respect to time |
| f | external input force |
| F | force |
| $F_A$ | attraction force |
| $F_g$ | gravitational force |
| $F_D$ | damping force |
| g | acceleration due to gravity |
| i | current |
| $i_0$ | equilibrium current |
| $\Delta I$ | *S*-domain small change in current |
| j | integer counter |
| k | integer counter |
| K | gain |
| $K_c$ | coil constant, $K_c = i_0 \frac{\partial L}{\partial x}\|_{x_0}$ |
| $K_d$ | derivative gain |
| $K_{in}$ | integral gain |
| $K_i$ | linearization constant, $K_i = \frac{\partial}{\partial i}(F_A)\|_{x_0, i_0}$ |
| $K_p$ | proportional gain |
| $K_x$ | linearization constant, $K_x = \frac{\partial}{\partial x}(F_A)\|_{x_0, i_0}$ |
| L | inductance |
| m | mass |
| n | high/low frequency gain |
| *p*,*P* | quadratic curve coefficient |
| *q*,*Q* | quadratic curve coefficient |
| *r*,*R* | quadratic curve coefficient |

| | |
|---|---|
| R | resistance |
| r | reference input |
| s | simulation time, seconds |
| $S$ | Laplace variable |
| T | time step, sampling period |
| t | time |
| V | voltage |
| $V_0$ | equilibrium voltage |
| $\Delta V$ | $S$-domain small change in voltage |
| V, $V'$ | output from controller |
| W | weighting factor |
| x | position, separation distance |
| $x_k$ | present position |
| $x_0$ | equilibrium position |
| $\dot{x}$ | first derivative of position, velocity |
| $\ddot{x}$ | second derivative of position, acceleration |
| $\Delta X$ | $S$-domain small change in position |
| y | state space output |
| y, $y'$ | intermediate controller calculation |
| $z$ | $z$-transformation variable |
| $\infty$ | infinity |
| $\epsilon$, $\epsilon'$ | input to controller |
| $\dot{\epsilon}$ | first derivative of input to controller |
| $\tilde{\epsilon}$ | intermediate controller calculation |
| $\epsilon_k$ | present input to controller |
| $\zeta$ | strike time step forward |
| $\delta$ | small variation in parameter |
| $\frac{\partial}{\partial x}$ | partial derivative with respect to x |
| $\frac{\partial}{\partial i}$ | partial derivative with respect to i |

## NOMENCLATURE

| | |
|---|---|
| D P A | Dual Phase-Advance |
| MIT | Massachusetts Institute of Technology |
| MSBS | Magnetic Suspension and Balance System |
| MSBSs | Magnetic Suspension and Balance Systems |
| NAL | National Aerospace Laboratory, Japan |
| NASA | National Aeronautics and Space Administration, United States |
| ONERA | Office National d'Etudes et de Recherches Aérospatiales, France |
| P D | Proportional Derivative |
| P I D | Proportional Integral Derivative |
| UVa | University of Virginia |

## LIST OF TABLES


| Table | | Page |
|---|---|---|
| 1. | Existing MSBS wind tunnels | 3 |
| 2. | Digital controllers for MSBS wind tunnels | 27 |
| 3. | Digital controllers for magnetic suspension systems | 38 |
| 4. | P I D controller location. (Position input) | 46 |
| 5. | D P A controller location. (Position input) | 48 |
| 6(a). | D P A, 5% overshoot. (Position input) | 51 |
| 6(b). | D P A, 5% overshoot. (Force input) | 51 |
| 7(a). | D P A, minimum first overshoot. (Position input) | 52 |
| 7(b). | D P A, minimum first overshoot. (Force input) | 52 |
| 8. | D P A relative execution times | 54 |
| 9(a). | P I D, minimum first overshoot. (Position input) | 56 |
| 9(b). | P I D, minimum first overshoot. (Force input) | 57 |
| 10. | P I D relative execution times | 59 |

## LIST OF FIGURES


| Figure | | Page |
|---|---|---|
| 1. | Schematic of single degree-of-freedom MSBS | 4 |
| 2. | Magnetic force - distance characteristics at constant current | 5 |
| 3. | Magnetic force - current characteristics at constant body position | 6 |
| 4. | Inductance - body position characteristics at constant current | 10 |
| 5. | Block diagram of MSBS plant | 12 |
| 6. | Location of MSBS plant poles in the complex plane | 13 |
| 7. | MSBS control loop | 16 |
| 8. | Magnetic force - distance characteristics as modified by the controller | 17 |
| 9. | Root locus of MSBS with phase advance controller | 18 |
| 10. | Root locus of MSBS with P I D controller | 19 |
| 11. | Sample timing for quadratic curve algorithm | 28 |
| 12. | Position trajectories of P I D, (controller location) | 45 |
| 13. | Position trajectories of D P A, (controller location) | 47 |
| 14. | Position trajectories of D P A controllers, 5% overshoot | 50 |
| 15. | Position trajectories of D P A controllers, minimum first overshoot | 53 |
| 16. | Position trajectories of P I D controllers, minimum first overshoot | 58 |

# 1. INTRODUCTION

The first recorded use of an actively stabilized magnetic suspension system was at the University of Virginia, USA, in 1937 (Ref. 1). Such systems are now finding many uses, including the suspension of models in wind tunnels.

Magnetic suspension of a model in a wind tunnel was first achieved in 1957 by researchers at the Office National d'Etudes et de Recherches Aérospatiales (ONERA), France (Ref. 2). The ONERA system controlled models in five degrees-of-freedom in test sections up to 30 cm in diameter. So far as is known, 17 wind tunnel magnetic suspension systems have been built since then, with six now in operation (Ref. 3, 4).

All wind tunnel magnetic suspension and balance systems (MSBSs) use controlled dc electromagnets acting on a suspended body containing a ferromagnetic material. With this approach, stabilization of the position and attitude of the suspended body requires feedback controllers. Early control systems used analog circuits, each individually designed for a particular system. Performance was restricted by practical limits on complexity and adjustment of the controller parameters, and stability of the analog elements. With the development of digital computers, digital control became possible, promising many advantages.

One advantage of a digital controller is that it requires less hardware than an analog controller. A digital controller uses digital-to-analog (DAC) and analog-to-digital converters (ADC) for communication between the computer and the MSBS. The control strategy is written in software and is easily modified to improve control techniques, either as better computer systems become available, or the MSBS changes. With a digital controller

the possibilities of controllers are limitless and the great flexibility of software allows complex control strategies.

Of the six known wind tunnels using magnetic suspension and balance systems, two are at NASA Langley Research Center in the USA. The others are at Oxford University and the University of Southampton in England, the National Aerospace Laboratory (NAL) in Japan, and The Central Aero-Hydrodynamics Institute (TsAGI) in the Soviet Union.

All of the existing MSBSs are fitted to relatively small wind tunnels. The largest system, which is in the Soviet Union, installed in a 40 x 60 cm test section and is used for low speed aerodynamic testing (Ref. 5). Both of the MSBSs in the USA are fitted to low speed atmospheric fan-driven open-return tunnels. One of the USA MSBS wind tunnels has a 15 cm diameter octagonal test section. The other, known as the Langley 13 inch MSBS, has a 26.7 x 31.8 cm octagonal test section and is used on a fairly regular basis for low speed aerodynamic testing. The MSBS at Oxford is fitted to a 12 x 12 cm hypersonic tunnel. The most highly developed MSBS is at the University of Southampton. The Southampton system is fitted to an 18 cm octagonal test section and is used for dynamic as well as static aerodynamic testing. The newest MSBS is the NAL system which is fitted to the 10 x 10 cm transonic test section of their Pilot Cryogenic Wind Tunnel.

Of these six MSBSs, only three are digitally controlled. These are the University of Southampton MSBS, the NASA Langley 13 inch MSBS, and the NAL MSBS. The Southampton MSBS digitally controls 10 electromagnets using a minicomputer to maintain control of the model in six degrees of freedom. The NASA Langley 13 inch system has only 5 electromagnets controlling five degrees of freedom. The NAL system controls five degrees-of-freedom using 10 electromagnets.

Table 1 gives a complete listing of the existing MSBS wind tunnels.

Table 1. Existing MSBS wind tunnels.

| Organization | Degrees of Freedom | Size, cm | Controller |
|---|---|---|---|
| TsAGI | 5 | 40 x 60 | analog |
| NASA Langley | 5 | 26.7 x 31.8 | digital |
| NASA Langley | 5/6 | 15 oct. | analog |
| Oxford University | 3 | 12 x 12 | analog |
| University of Southampton | 5/6 | 18 oct. | digital |
| NAL | 5 | 10 x 10 | digital |

## 2. GOVERNING EQUATIONS

The principles of an MSBS can be understood by studying a single degree-of-freedom system. Figure 1 shows a simple single degree-of-freedom MSBS consisting of a dc electromagnet and a suspended magnetic body. The suspended body must contain some ferromagnetic material. The electromagnetic field from the coil produces a magnetic force which attracts the suspended body to the coil. Gravity acts to pull the suspended body away from the coil. If the current in the coil increases, the magnetic force of attraction also increases.

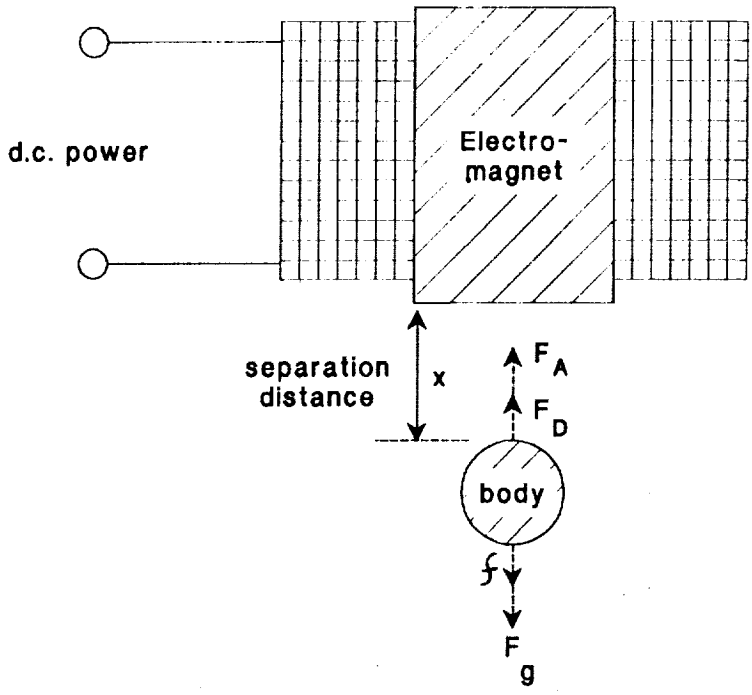


Figure 1. Schematic of single degree-of-freedom MSBS.

As shown in figure 2, for constant coil current, the magnetic force attracting the body decreases as the separation distance, x, increases. This decrease in the magnetic force attracting the body as the separation distance increases makes this system inherently unstable. Because this system is inherently unstable, a feedback control system is required to regulate the coil current. The control system must increase the current when the separation distance increases and reduce the current when the separation decreases. Stable suspension of the body is possible through proper regulation of the current by the controller.

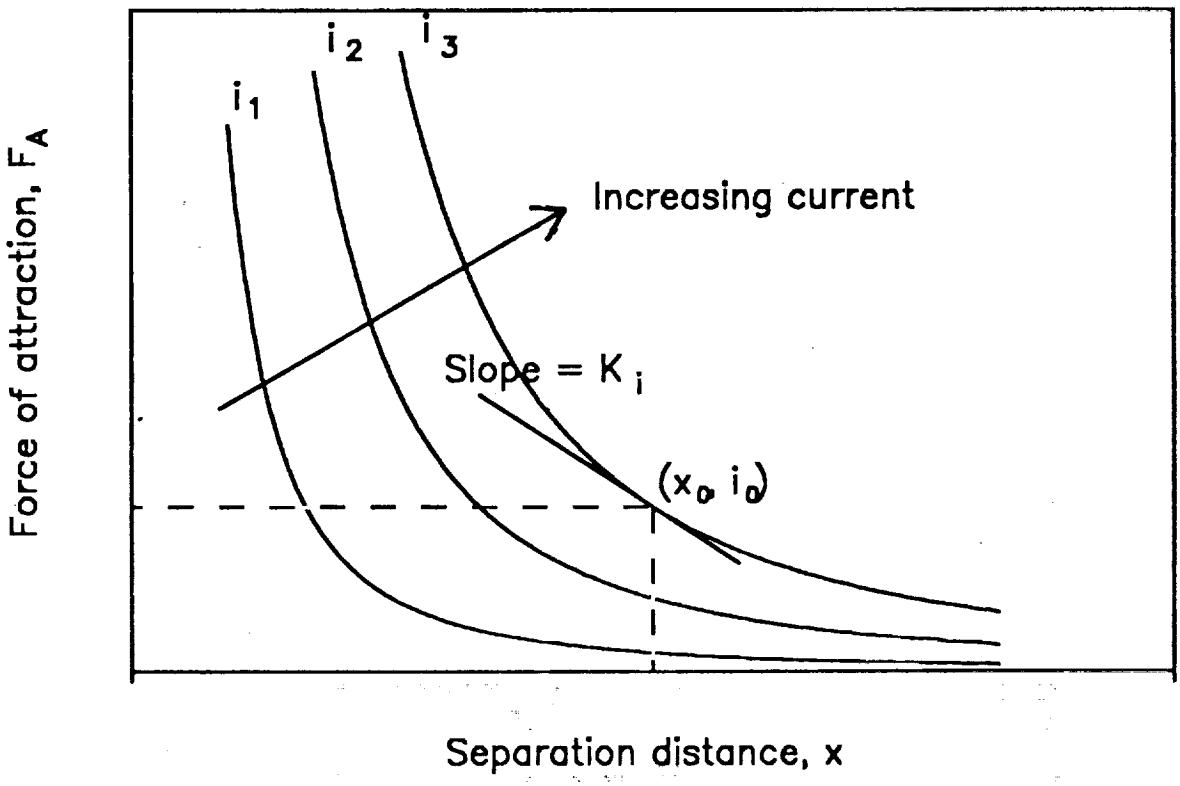


Figure 2. Magnetic force - distance characteristics at constant current.

## 2.1 Dynamics of the Suspended Body

The equation of motion for the suspended body is derived from Newton's second law of motion.

$$m \ddot{x} = \sum F$$

Neglecting bouyancy, there are four forces acting on the suspended body in a single degree-of-freedom system as shown in figure 1. These forces are gravity, the magnetic force produced by the coil, a damping force, and any external force acting on the body. Taking positive x in the direction of gravity, the equation of motion for the body is:

$$m \ddot{x} = F_g - F_A(x, i) - F_D + f \tag{2.1}$$

In equation 2.1, $F_g$ is the weight of the body, $F_A$ is the magnetic force exerted on the body by the coil, $F_D$ is the damping force acting on the body, and f is an external force.

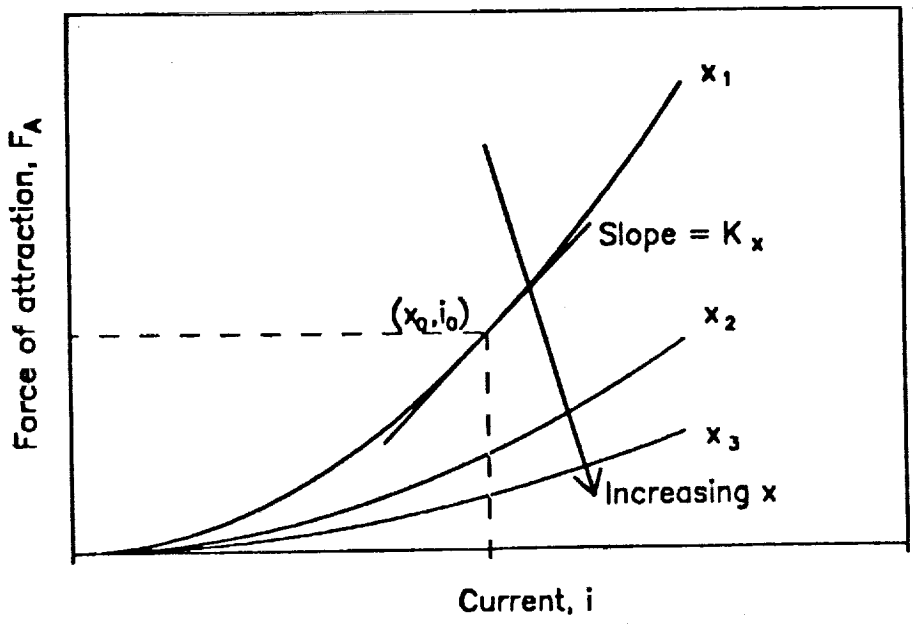


Figure 3.- Magnetic force - current characteristics at constant body position.

The magnetic force $F_A$, is usually nonlinear. It is a function of the current in the coil and the position of the suspended body. Figures 2 and 3 show how this magnetic force varies with coil current and position of the body. The variation in force with x and i may be linearized by limiting the motion of the body and the current in the coil to small variations around their equilibrium values. (Ref. 6, 7)

Let $i(t) = i_0+\delta i(t)$ where $i_0$ is a constant current and $\delta i(t)$ is a small time-dependent variation in current around $i_0$. Let $x(t) = x_0+\delta x(t)$ where $x_0$ is an equilibrium position and $\delta x(t)$ is a small variation in position around $x_0$. Therefore:

$$F_A = F(x_0, i_0) + \frac{\partial}{\partial x}(F_A)\Big|_{x_0,\, i_0} \delta x(t) + \frac{\partial}{\partial i}(F_A)_{x_0,\, i_0} \delta i(t) + \text{higher order terms} \qquad (2.2)$$

$F(x_0, i_0)$ is the magnetic force of attraction caused by the current $i_0$ with the body at an equilibrium point $x_0$. The partial derivatives of $F_A$ are the slopes of the force curves for constant current and constant position. Under equilibrium conditions, $F(x_0, i_0)$ is the magnetic force required to exactly balance the gravitational force acting on the body and any external forces which are constant. Therefore:

$$F(x_0, i_0) = F_g = mg + f_{constant}$$

For small variations in current and position, let $\frac{\partial}{\partial x}(F_A)_{x_0,\, i_0} = K_X$ and $\frac{\partial}{\partial i}(F_A)_{x_0,\, i_0} = K_i$. Equation 2.2 is further simplified by neglecting as insignificant the higher order terms. As shown in figures 2 and 3, the slopes of the curves are such that $K_X$ is negative and $K_i$ is positive. These force constants can be considered to represent the spring-like stiffness of the system. These force constants can be determined experimentally for a given equilibrium current and position.

Equation 2.1 takes account of the damping forces acting on the body caused by both aerodynamic (viscous) and eddy current damping. These damping forces are assumed to be velocity dependent. The eddy current damping is usually very small and can be ignored. However, the aerodynamic damping can be large, especially for wind tunnel testing. The damping term has a negative sign because the damping force always opposes the motion. A motion in the positive direction produces a damping force in the negative direction and a motion in the negative direction produces a damping force in the positive direction. With small variations in position, the damping force becomes:

$$F_D = C\,\dot{x}$$

The linearized equation of motion for the suspended body about an equilibrium point is:

$$m\,\delta\ddot{x}(t) = K_x\,\delta x(t) - K_i\,\delta i(t) - C\,\delta\dot{x}(t) + f \tag{2.3}$$

In this equation 2.3, f is the change in external force.

## 2.2 Governing Equation of the Magnetic Coil

The governing equation of the electromagnetic coil is the sum of the voltage drop across the coil resistance and the voltage across the electromagnetic coil.

$$V(t) = i(t)\,R + \frac{d}{dt}\Big(i(t)\,L\Big) = i(t)\,R + L\,\frac{d}{dt}\Big(i(t)\Big) + i\,\frac{d}{dt}(L) \tag{2.4}$$

Where V(t) is voltage, i(t) is current, L is inductance, and R is resistance.

In addition to being a function of the geometry of the coil, the inductance of the coil is a function of the suspended objects position, L = L(x). The time rate of change of the inductance

can be simplified by invoking the chain rule, $\frac{d}{dt}(L(x)) = \frac{d}{dx}(L)\,\frac{d}{dt}\left(x(t)\right)$. Substituting this in equation 2.4 gives:

$$V(t) = i(t)\,R + L\,\frac{d}{dt}\left(i(t)\right) + i(t)\,\frac{d}{dx}(L)\,\frac{d}{dt}\left(x(t)\right) \tag{2.5}$$

This velocity, $\frac{d}{dt}\left(x(t)\right)$, is caused by changes in the inductance L, resulting from the motion of the body. This velocity is not related to a change in coil current. (Ref. 8)

One method of linearizing equation 2.5 is to assume V(t), i(t), and x(t) are allowed only small variations around some equilibrium points as assumed in the equation of motion for the suspended body. For small variations, $V(t) = V_0+\delta V(t)$, $i(t) = i_0+\delta i(t)$, and $x(t) = x_0+\delta x(t)$. Substitution of these expressions into equation 2.5 gives:

$$V_0+ \delta V(t) = \left(i_0 + \delta i(t)\right)R + L\,\frac{d}{dt}\left(i_0 + \delta i(t)\right) + \left(i_0 + \delta i(t)\right)\frac{d}{dx}(L)\,\frac{d}{dt}\left(x_0+\delta x(t)\right)$$

$$V_0+ \delta V(t) = i_0\,R + \delta i(t)\,R + L\,\frac{d}{dt}\left(\delta i(t)\right) + i_0\,\frac{d}{dx}(L)\,\delta\dot{x}(t) + \delta i(t)\,\frac{d}{dx}(L)\,\delta\dot{x}(t) \tag{2.6}$$

Since $V_0 = i_0\,R$, this becomes:

$$\delta V(t) = \delta i(t)\,R + L\,\frac{d}{dt}\left(\delta i(t)\right) + i_0\,\frac{d}{dx}(L)\,\delta\dot{x}(t) + \delta i(t)\,\frac{d}{dx}(L)\,\delta\dot{x}(t) \tag{2.7}$$

If $\delta i(t)$ and $\delta\dot{x}(t)$ are very small, then their product is even smaller and can be neglected as insignificant. Equation 2.7 is further simplified by letting $i_0\frac{d}{dx}(L)|_{x_0} = K_c$ because $\frac{d}{dx}(L)$ is a constant slope for small changes in position as shown in figure 4.

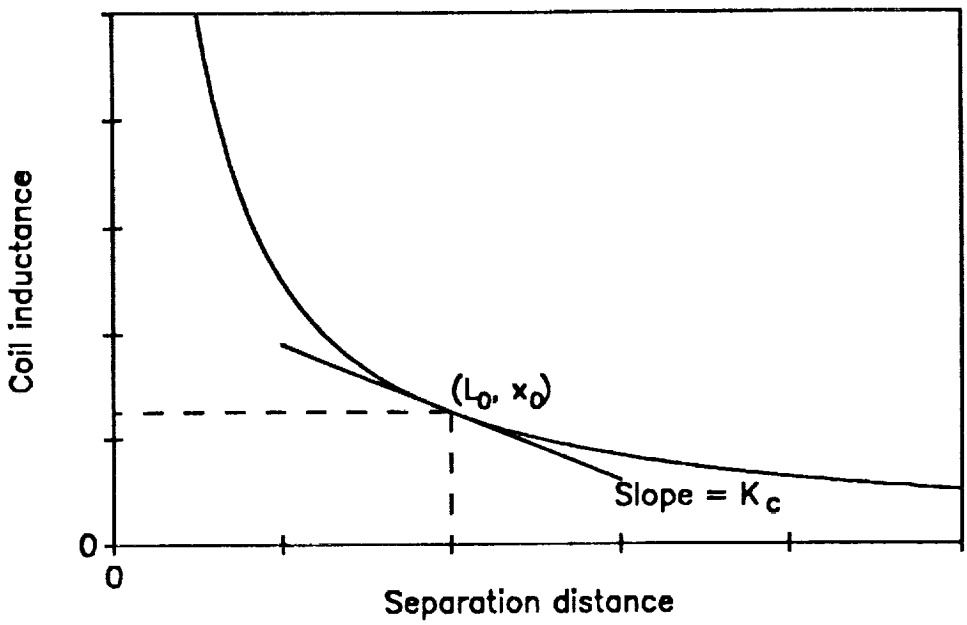


Figure 4. Induction - body position characteristics at constant current.

Therefore the linearized approximation of equation 2.4 is:

$$\delta V(t) = \delta i(t)\, R + L \frac{d}{dt}\Big(\delta i(t)\Big) + K_c\, \delta \dot{x}(t) \tag{2.8}$$

## 2.3 Single Degree-of-Freedom MSBS Transfer Function

The system differential equations for small variations are equations 2.3 and 2.8.

$$m\, \delta \ddot{x}(t) = K_x\, \delta x(t) - K_i\, \delta i(t) - C\, \delta \dot{x}(t) + f \tag{2.3}$$

$$\delta V(t) = \delta i(t)\, R + L \frac{d}{dt}\Big(\delta i(t)\Big) + K_c\, \delta \dot{x}(t) \tag{2.8}$$

Assuming the initial conditions are zero, these equations transfer to the Laplacian $S$-domain as:

$$m\, S^2 \Delta X = K_x\, \Delta X - K_i\, \Delta I - C\, S \Delta X + f \qquad \Delta V = \Delta I\, R + L\, S \Delta I + K_c\, S \Delta X$$

$$\Big(m\, S^2 + C\, S - K_x\Big)\, \Delta X = - K_i\, \Delta I + f \qquad \Delta V = \Delta I \Big(R + L\, S\Big) + K_c\, S \Delta X$$

$$\Delta X(m\,S^2 + C\,S - K_x) = -K_i \Delta I + f \qquad \Delta I = \frac{\Delta V - K_c S\,\Delta X}{R + L\,S} \qquad (2.9a, b)$$

$$\Delta X \left(S^2 + \frac{C}{m} S - \frac{K_x}{m}\right) = \frac{-K_i}{m} \Delta I + \frac{f}{m} \qquad \Delta I = \frac{\frac{\Delta V}{R} - \frac{K_c}{R} S\,\Delta X}{\left(1 + \frac{L}{R} S\right)}$$

$$\Delta X \left(S^2 + \frac{C}{m} S - \frac{K_x}{m}\right) = \frac{\frac{-K_i}{m\,R}}{\left(1 + \frac{L}{R} S\right)} \Delta V + \frac{\frac{K_i\,K_c}{m\,R}}{\left(1 + \frac{L}{R} S\right)} S\,\Delta X + \frac{f}{m}$$

$$\Delta X \left\{S^2 + \left(\frac{C}{m} - \frac{K_i\,K_c}{m\,R\left(1 + \frac{L}{R} S\right)}\right) S - \frac{K_x}{m}\right\} = \frac{\frac{-K_i}{m\,R}}{\left(1 + \frac{L}{R} S\right)} \Delta V + \frac{f}{m}$$

Combining equations 2.9a and 2.9b gives the transfer function of this single degree-of-freedom system (in control nomenclature, this is referred to as the *plant transfer function*):

$$\Delta X = \frac{\frac{-K_i}{m\,R} \Delta V + \frac{f}{m}\left(1 + \frac{L}{R} S\right)}{\left(1 + \frac{L}{R} S\right)\left\{S^2 + \left(\frac{C}{m} - \frac{K_i\,K_c}{m\,R\left(1 + \frac{L}{R} S\right)}\right) S - \frac{K_x}{m}\right\}} \qquad (2.10a)$$

$$\Delta X = \frac{\frac{-K_i}{m\,R} \Delta V}{\left(1 + \frac{L}{R} S\right)\left\{S^2 + \left(\frac{C}{m} - \frac{K_i\,K_c}{m\,R\left(1 + \frac{L}{R} S\right)}\right) S - \frac{K_x}{m}\right\}}$$

$$+ \frac{\frac{f}{m}}{\left\{S^2 + \left(\frac{C}{m} - \frac{K_i\,K_c}{m\,R\left(1 + \frac{L}{R} S\right)}\right) S - \frac{K_x}{m}\right\}}$$

$$\Delta X = \frac{\frac{-K_i}{m\,L}\,\Delta V + \frac{R}{m\,L}\left(1 + \frac{L}{R}\,S\right) f}{S^3 + S^2\left(\frac{R}{L} + \frac{C}{m}\right) + S\left(\frac{C\,R}{m\,L} - \frac{K_x}{m} - \frac{K_i\,K_c}{m\,L}\right) - \frac{R\,K_x}{L\,m}} \qquad (2.10b)$$

A block diagram of this plant is shown in figure 5.

For the system with no change in external force inputs, f=0, there are three poles. The poles are coupled as seen in equation 2.10a. The pole located at -R/L is the lag time created by the power supply and electromagnetic coil.

The other two poles depend on the constants associated with the MSBS and the lag time. Typically these two poles are paired in the complex plane with a pole to the right and a pole to the left of the imaginary axis. The positive pole causes the system to be unstable.

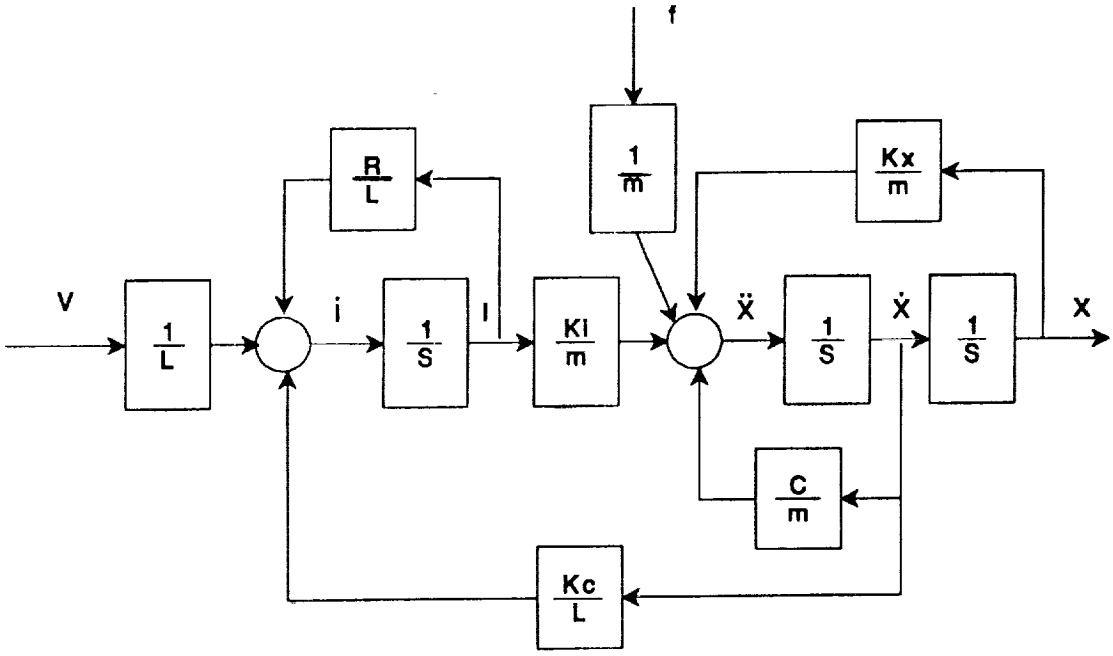


Figure 5. Block diagram of MSBS plant.

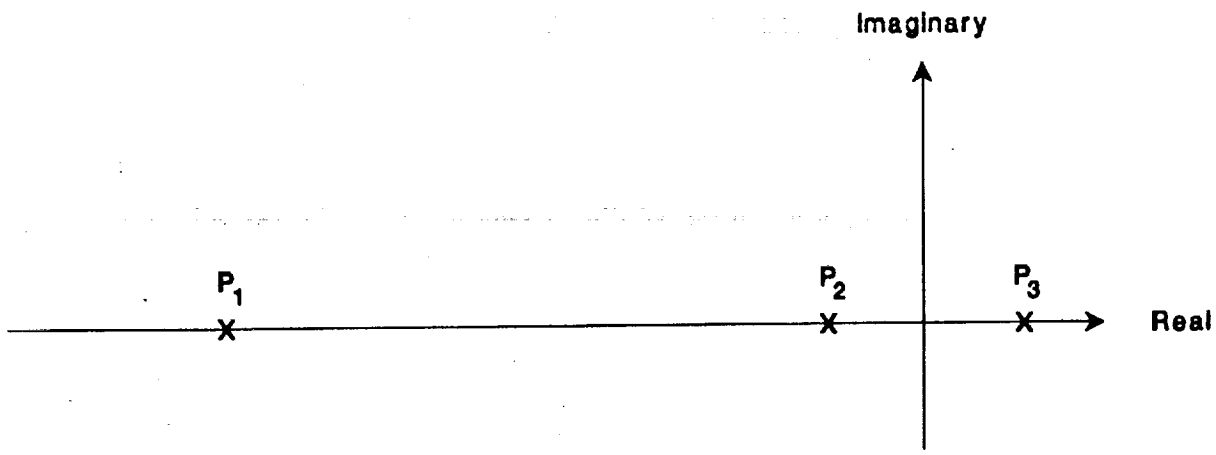


Figure 6. Location of MSBS plant poles in the complex plane.

Figure 6 shows the pole locations of a linearized MSBS plant. By observing the effects the system parameters have on the pole locations, it is possible to modify the design of a MSBS to position the poles.

The resistance of the coil, R, has a large influence on the location of the pole $P_1$. Increasing R will move $P_1$ to the left in the complex plane. Increasing R will also move $P_2$ slightly to the left and $P_3$ slightly to the right.

The inductance of the coil, L, also has a large influence on the location of $P_1$. Increasing L moves $P_1$ to the right in the complex plane. Increasing L will also move $P_2$ slightly to the right and $P_3$ slightly to the left.

The negative value of $K_X$ is the primary reason for the instability of a MSBS. Increasing the negative value of $K_X$ causes the poles $P_1$ and $P_2$ to move to the left while moving pole $P_3$ to the right.

Increasing the damping coefficient, C, moves the poles $P_1$ and $P_3$ to the left and $P_2$ to the right. This increased aerodynamic damping usually increases the stability of the MSBS.

Another parameter often available during the design of a MSBS is the mass, m, of the suspended body. Increasing the mass moves the poles $P_1$ and $P_2$ to the right, and pole $P_3$ to the left.

The constants $K_i$ and $K_c$ will shift the poles in the same directions. Increasing $K_i$ or $K_c$ causes pole $P_1$ to move left, and poles $P_2$ and $P_3$ to move right.

## 2.4 State Space Representation

The system differential equations with a small input force disturbance, f, are:

$$\delta\ddot{x}(t) = \frac{K_x}{m}\,\delta x(t) - \frac{K_i}{m}\,\delta i(t) - \frac{C}{m}\,\delta\dot{x}(t) + \frac{f}{m}$$

$$\delta\dot{i}(t) = \frac{1}{L}\delta V(t) - \frac{R}{L}\,\delta i(t) - \frac{K_c}{L}\,\delta\dot{x}(t)$$

By choosing the state variables as $\delta x$, $\delta\dot{x}$, and $\delta\dot{i}$, the state-space form is:

$$\begin{bmatrix} \delta x \\ \delta\dot{x} \\ \delta\dot{i} \end{bmatrix} = \begin{bmatrix} 0 & 1 & 0 \\ \frac{K_x}{m} & \frac{-C}{m} & \frac{-K_i}{m} \\ 0 & \frac{-K_c}{L} & \frac{-R}{L} \end{bmatrix} \begin{bmatrix} \delta x \\ \delta\dot{x} \\ \delta i \end{bmatrix} + \begin{bmatrix} 0 & 0 \\ 0 & \frac{1}{m} \\ \frac{1}{L} & 0 \end{bmatrix} \begin{bmatrix} \delta V \\ f \end{bmatrix} \qquad (2.11)$$

$$y = \begin{bmatrix} 1 & 0 & 0 \end{bmatrix} \begin{bmatrix} \delta x \\ \delta\dot{x} \\ \delta i \end{bmatrix}$$

For f=0 the system equations are:

$$\delta\ddot{x}(t) = \frac{K_x}{m}\,\delta x(t) - \frac{K_i}{m}\,\delta i(t) - \frac{C}{m}\,\delta\dot{x}(t) \qquad \delta\dot{i}(t) = \frac{1}{L}\delta V(t) - \frac{R}{L}\,\delta i(t) - \frac{K_c}{L}\,\delta\dot{x}(t)$$

and the state-space representation is:

$$\begin{bmatrix} \delta\dot{x} \\ \delta\ddot{x} \\ \delta\dot{i} \end{bmatrix} = \begin{bmatrix} 0 & 1 & 0 \\ \frac{K_x}{m} & \frac{-C}{m} & \frac{-K_i}{m} \\ 0 & \frac{-K_c}{L} & \frac{-R}{L} \end{bmatrix} \begin{bmatrix} \delta x \\ \delta\dot{x} \\ \delta i \end{bmatrix} + \begin{bmatrix} 0 \\ 0 \\ \frac{1}{L} \end{bmatrix} \begin{bmatrix} \delta V \end{bmatrix} \tag{2.12}$$

$$y = \begin{bmatrix} 1 & 0 & 0 \end{bmatrix} \begin{bmatrix} \delta x \\ \delta\dot{x} \\ \delta i \end{bmatrix}$$

This state-space representation can be shown to be controllable and observable. Because this system is controllable and observable, state-space control laws can be used to control the system. With a state-space controller the poles of the controlled system can be positioned at any desired location in the complex plane.

## 3. MAGNETIC SUSPENSION AND BALANCE SYSTEM CONTROLLERS

The typical MSBS is a multiple degree-of-freedom system using, as a minimum, one electromagnetic coil for each degree-of-freedom controlled.

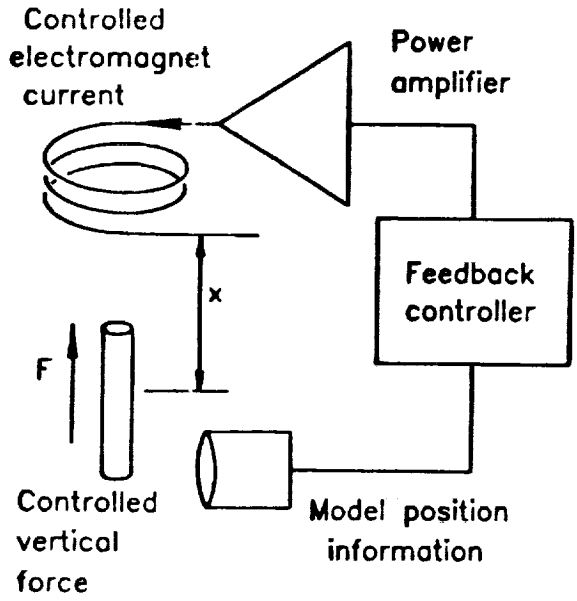


Figure 7. MSBS control loop.

The controller in an MSBS used with a wind tunnel must stabilize and control the axial, lateral, and heave (x, y, z) positions and the roll, pitch, and yaw ($\phi$, $\theta$, $\psi$) orientations of the suspended model (although roll is often left open-loop). This requires continuous adjustment of the currents in the electromagnetic coils. The adjustments of the coil currents must modify the attraction force curve in figure 3 to that shown in figure 8 below. (Ref. 9)

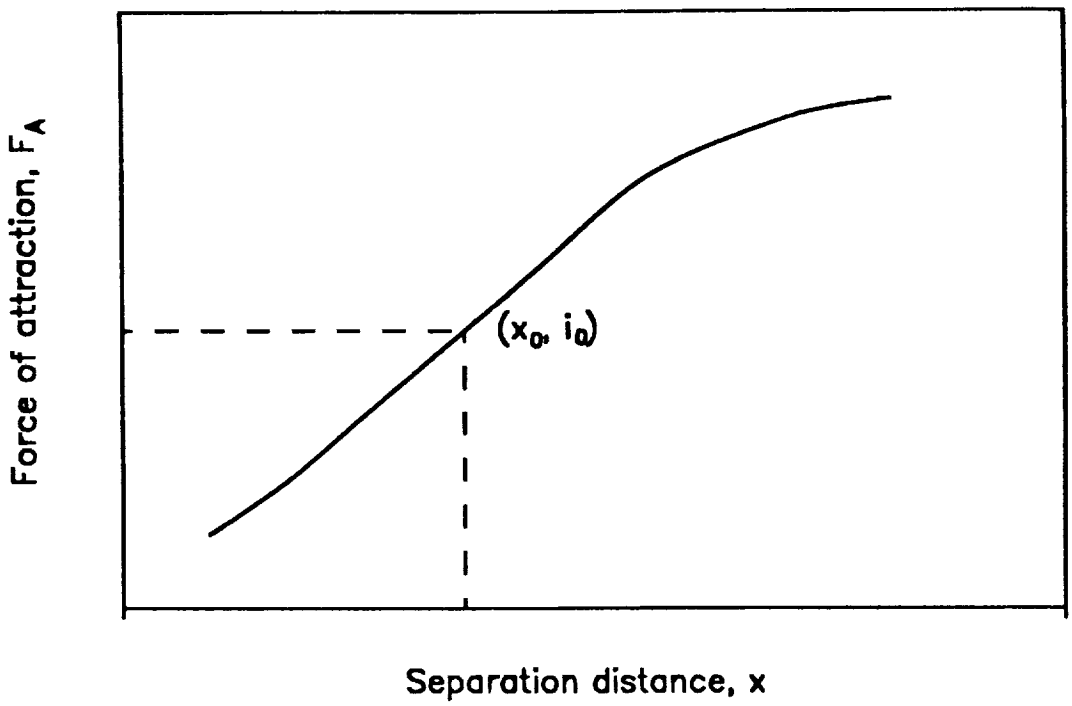


Figure 8. Magnetic force - distance characteristics as modified by the controller.

From the plant transfer function given in equation 2.10, it can be seen that the system is inherently unstable. A position feedback is insufficient to achieve stability, therefore some form of rate information is necessary (Ref. 10).

Because position information is usually available, the traditional approach for an MSBS controller is to generate limited rate information (position derivatives) using analog phase-advance controllers, proportional-derivative controllers, or a proportional-integral-derivative controllers, often combined with error integrators to minimize steady-state errors. The controller is located either in the forward path or the feedback path.

### 3.1 Phase Advance Controller

The standard form of a phase-advance controller is:

$$\text{input} \rightarrow \left[\frac{1+ A\ S}{1+ B\ S}\right] \rightarrow \text{output} \tag{3.1}$$

Where A and B are the phase-advance time constants and the ratio of A/B is the high-low frequency gain.

A single phase-advance can be adequate for some systems, although two or more are usually combined in series. The values of A and B would depend on the pole locations of an MSBS plant and the desired system performance.

A single phase-advance has one pole and one zero. The pole and zero of the phase-advance controller should be located so they affect the stability of the MSBS plant. The idea is to choose a zero for the phase-advance which will make the system stable. Figure 9 shows the modifications that a phase-advance makes to the root locus, giving the system a stability range. The actual location of the pole and zero will be based on the plant poles and the desired system performance.

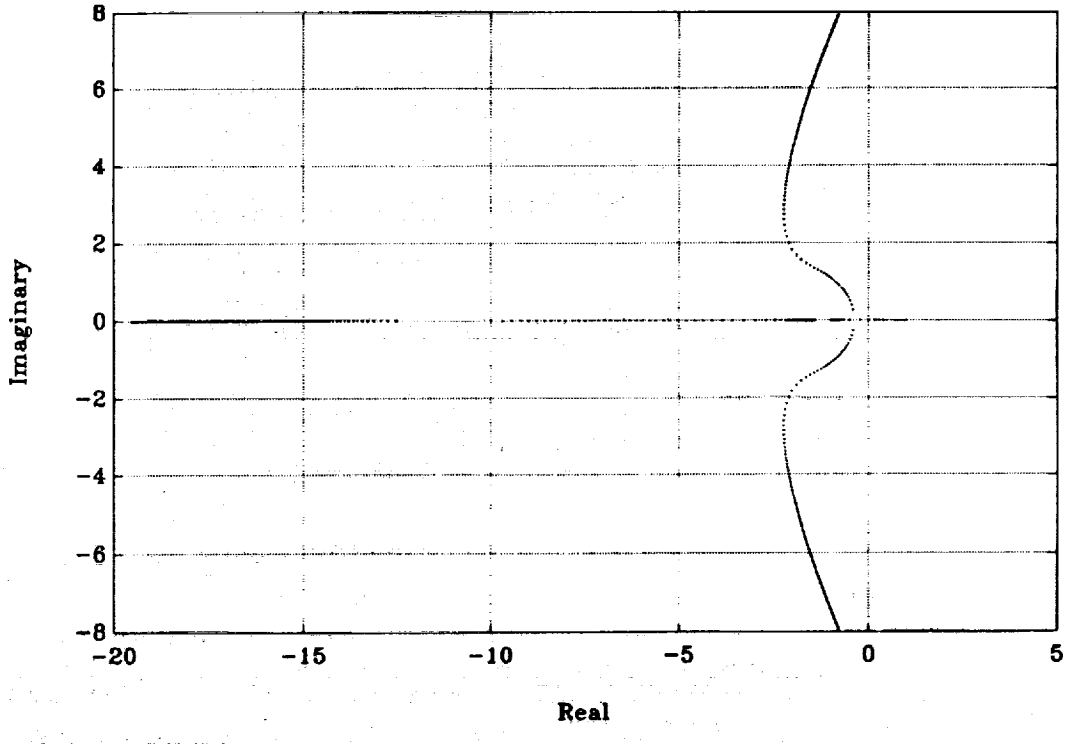


Figure 9. Root locus of MSBS with phase-advance controller.

### 3.2 Proportional-Integral-Derivative Controller

The standard form of a proportional-integral-derivative (P I D) controller is:

$$\text{input} \rightarrow \left[ K_p + K_d S + \frac{K_{in}}{S} \right] \rightarrow \text{output} \tag{3.2}$$

This controller will have a pole located at the origin of the complex plane and two zeros to the left of the imaginary axis. Again, the location of the zeros can be selected to provide a range of stability for the system. Figure 10 shows how a P I D controller modifies the root locus of the MSBS plant.

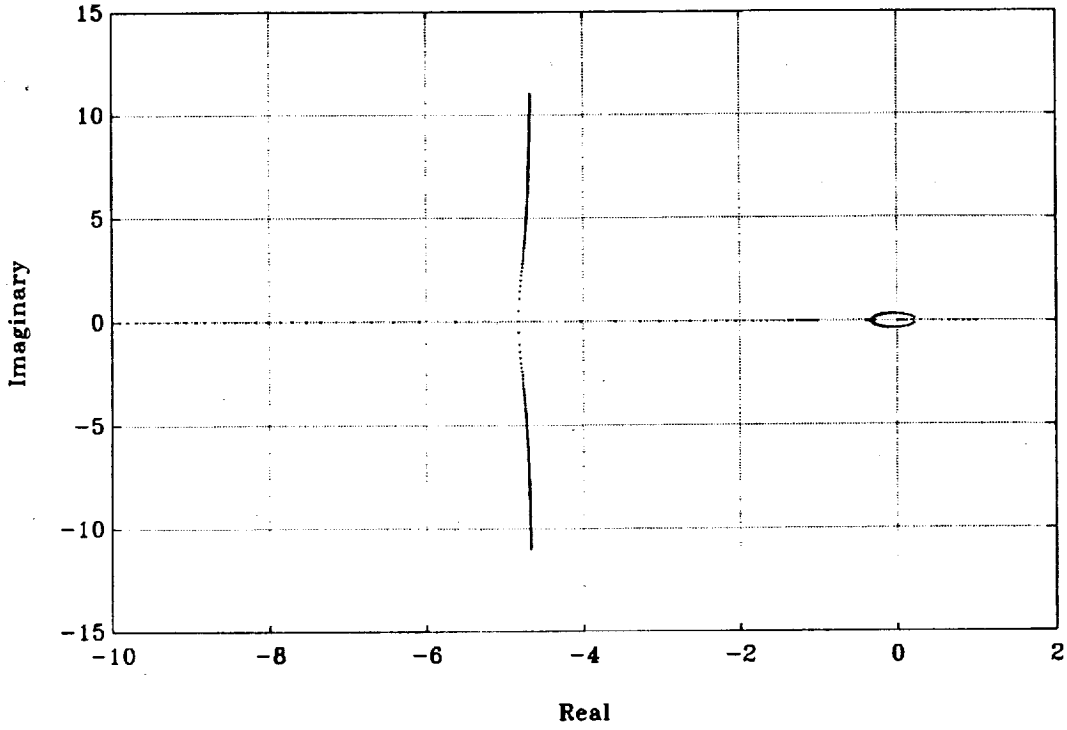


Figure 10. Root locus of MSBS with P I D controller.

# 4. CONTROLLERS

## 4.1 Development of Digital Controllers for Wind Tunnel MSBSs

The use of digital controllers in MSBSs allows an infinite number of possibilities for controllers. The first attempts at using digital controls were simply to simulate existing analog control systems. The approach of digitally simulating the analog controller can be simple or complex as shown for the following MSBS digital control systems. The sections which follow present a chronological history of the development of digital controllers for wind tunnels.

### 4.1.1 Oxford, England:

The development of digital control systems for an MSBS started in 1971 at Oxford University. The Oxford MSBS controller was implemented with conventional circuitry, using analog sample-and-hold stages. Discrete-time control was necessary due to the use of a scanning TV system for position detection of a small sphere (Ref. 11). Three degrees-of-freedom, the horizontal and vertical position, were controlled in the MSBS. Although it did not use a true digital controller, the work is noteworthy since it was founded on the same theoretical basis as later digital controllers. Furthermore, the system required a formidably complex piece of circuitry.

The control algorithm is derived from a $z$-transformation of a phase-advance controller. The phase-advance transfer function expands in the $z$-domain as:

$$\frac{V}{\epsilon} = K\left[\frac{1 + a_{-1}\, z^{-1} + a_{-2}\, z^{-2}}{1 + b_{-1}\, z^{-1} + b_{-2}\, z^{-2}}\right]$$

rewritten as a difference equation, this transfer function is:

$$V_k = K \left[ \epsilon_k + a_{-1}\, \epsilon_{k-1} + a_{-2}\, \epsilon_{k-2} - b_{-1}\, V_{k-1} - b_{-2}\, V_{k-2} \right]$$

The controller was located in the forward loop of the system. The output, $V_k$, is based on the previous and twice previous command signals and the present, previous, and twice previous error signals. The system used 100 control cycles per second.

This system was later developed to include an integrator in the forward path with combinations of phase-advance controllers (Ref. 12).

### 4.1.2 MIT, United States:

The next developments occurred at MIT in 1976, when the theoretical application of full digital controls to the MSBS was studied (Ref. 13). MIT developed a hybrid simulation of an MSBS using a microcomputer and an analog computer. A one degree-of-freedom demonstration system was digitally controlled using a $z$-transformation of a triple phase-advance controller on an INTEL 8080 microprocessor. The single degree-of-freedom triple phase-advance controller had the following form:

$$\frac{V}{\epsilon} = K \left[ \frac{(z-a_3)(z-a_2)(z-a_1)}{(z-b_3)(z-b_2)(z-b_1)} \right]$$

The researchers at MIT gave guidelines for the computing power required for a full MSBS system. However, financial support could not be obtained for further development of this system and the work was dropped.

### 4.1.3 Southampton, England:

In 1981, researchers at the University of Southampton developed a two degree-of-freedom digital controller for their MSBS (Ref. 14). Initially only vertical translation and pitch rotation were controlled by digitally simulating an analog dual phase-advance controller using a PDP-11/34 computer. The Southampton system placed the controller in the feedback path of the circuit and an error integrator in the forward path. The dual phase-advance transfer function is:

$$\frac{V}{\epsilon} = \left[\frac{(1+ nA\ S)^2}{(1+ B\ S)^2}\right]$$

The Southampton digital algorithm is derived from a difference equation approximation of the controller transfer function. The transfer function is split into four blocks where the third and fourth blocks are the same as blocks one and two. The phase-advance time constants A and B are equal. The n is a constant to obtain the desired high/low frequency gain, nA/B, for the phase-advance controller when A and B are equal.

$$\epsilon \rightarrow \left[\frac{1}{1+ A\ S}\right]_1 \rightarrow y \rightarrow [\,1+ nA\ S\,]_2 \rightarrow V' \rightarrow \epsilon' \rightarrow \left[\frac{1}{1+ A\ S}\right]_3 \rightarrow y' \rightarrow [\,1+ nA\ S\,]_4 \rightarrow V$$

The first two blocks were originally approximated as follows:

$$A\frac{\Delta y}{T} = \epsilon_k - y_{k-1} \qquad V'_k = y_k + nA\frac{\Delta y}{T}$$

where $\Delta y = y_k - y_{k-1}$

giving $y_k = \left(\frac{T}{A}\right)\epsilon_k + \left(\frac{A-T}{A}\right)y_{k-1}$ $\qquad V'_k = \left(\frac{T+nA}{T}\right)y_k - \left(\frac{nA}{T}\right)y_{k-1}$

If $a_1 = \frac{T}{A}$, $a_2 = \frac{A-T}{A}$, $a_3 = \frac{T+nA}{T}$, and $a_4 = \frac{-nA}{T}$ then these equations can be resolved into difference equations where:

$$y_k = a_1\epsilon_k + a_2 y_{k-1} \qquad V'_k = a_3 y_k + a_4 y_{k-1}$$

and

$$y_{k-1} = a_1\epsilon_{k-1} + a_2 y_{k-2} \qquad V'_{k-1} = a_3 y_{k-1} + a_4 y_{k-2}$$

then combined:

$$V'_k = a_2 V'_{k-1} + a_3 a_1 \epsilon_k + a_4 a_1 \epsilon_{k-1} \tag{4.1a}$$

Also from the third and fourth block:

$$V_k = a_2 V_{k-1} + a_3 a_1 \epsilon'_k + a_4 a_1 \epsilon'_{k-1} \tag{4.1b}$$

Assuming $V' = \epsilon'$ and combining equations 4.1a and 4.1b in series is then a difference approximation of a dual phase-advance. The values of the constants A, n, and T used were different for the two degrees-of-freedom. The system initially used 1500 control cycles per second and fixed point arithmetic programmed in assembly language. A sensitivity to input noise was discovered but these problems were overcome and development of a six degree-of-freedom digital controller began.

In 1984 a six degree-of-freedom digital controller was completed (Ref. 15). The system continued to use the digital phase-advance controller, with minor changes from the 1981 algorithm in the first and third blocks. These changes were:

$$\epsilon \rightarrow \left[ \frac{1}{1+A\,S} \right]_1 \rightarrow y$$

$$A\frac{\Delta y}{T} = \epsilon_k - y_k \quad \text{(previously: } A\frac{\Delta y}{T} = \epsilon_k - y_{k-1}\text{)}$$

where $\Delta y = y_k - y_{k-1}$

then $y_k = \left(\frac{T}{A+T}\right)\epsilon_k + \left(\frac{A}{A+T}\right) y_{k-1}$

These equations can also be reduced to difference equations as:

$$V'_k = a_2 V'_{k-1} + a_3 a_1 \epsilon_k + a_4 a_1 \epsilon_{k-1} \tag{4.2a}$$

$$V_k = a_2 V_{k-1} + a_3 a_1 \epsilon'_k + a_4 a_1 \epsilon'_{k-1} \tag{4.2b}$$

Here $a_1 = \frac{T}{A+T}$ and $a_2 = \frac{A}{A+T}$ which differ from equations 4.1a and 4.1b for the earlier systems.

This form was believed to give superior performance for long sampling intervals ($T \approx A$). As extra control tasks placed increased demands on the control system, increased processing capability was necessary. This was provided by replacing the PDP-11/34 with a PDP-11/84. The extra control tasks included position sensor processing and output demand distribution related to high angle of attack operation (Ref. 16). The control algorithm is in floating point assembly language and originally operated at 400 control cycles (all six degrees of freedom) per second. The controller now operates at 256 control cycles per second.

The error integrator used in the system is located in the forward path. The integrator in digital form is:

$$V_k = K_{in}\, T \sum_{j=0}^{k} \epsilon_j \tag{4.3}$$

The error integrator drives the steady-state error to zero.

#### 4.1.4 NASA Langley, United States:

In 1984 the NASA Langley Research Center 13-inch MSBS was converted to digital controls (Ref. 17). The controller closely followed the Southampton system, using a PDP-11/23 computer to control five degrees-of-freedom (no roll control). With the same control loop configuration, the algorithm was modified slightly from the Southampton version to save time in execution (eliminated one floating point multiplication):

$$\epsilon \rightarrow \left[\frac{T}{A}\right] \rightarrow \tilde{\epsilon} \rightarrow \left[\frac{A}{T(1+\Lambda S)}\right] \rightarrow y \rightarrow [\,1+ n\Lambda\, S\,] \rightarrow V'$$

where $y_k = \frac{A}{T+A}[\tilde{\epsilon}_k + y_{k-1}]$ and $V'_k = (1+\frac{n\Lambda}{T})\, y_k - \frac{n\Lambda}{T}\, y_{k-1}$

This allows the entire dual phase-advance transfer function to be rearranged as:

$$\epsilon \rightarrow \left[\frac{T^2}{A^2}\right] \rightarrow \tilde{\epsilon} \rightarrow \left[\frac{A}{T(1+\Lambda S)}\right] \rightarrow y \rightarrow [1+ n\Lambda\, S] \rightarrow V' \rightarrow \left[\frac{A}{T(1+\Lambda S)}\right] \rightarrow y' \rightarrow [1+ n\Lambda\, S] \rightarrow V$$

This can be expressed as three equations applied in series as:

$$\tilde{\epsilon} = a_2\,\epsilon \tag{4.4a}$$

$$V'_k = a_3 a_1 \tilde{\epsilon}_k + a_1 a_4 \epsilon_{k-1} + a_1 V'_{k-1} \tag{4.4b}$$

$$V_k = a_1 a_3 V'_k + a_1 a_4 V'_{k-1} + a_1 V_{k-1} \tag{4.4c}$$

where, $a_1 = \frac{A}{T+A}$, $a_2 = \frac{T^2}{A^2}$, $a_3 = \frac{T+nA}{T}$, and $a_4 = \frac{-nA}{T}$

The NASA controller uses floating point assembly language and a controller operating at 256 cycles per second.

### 4.1.5 NAL, Japan:

The newest MSBS was commissioned at the National Aerospace Laboratory, Tokyo, Japan in 1987, with digital controls used from the outset. Few details of the controller are available. However, the system appears to use some form of digital approximation of a classical P I D algorithm carried out on a microcomputer.

$$\frac{V}{\epsilon} = \left[ K_p + K_d S + \frac{K_{in}}{S} \right]$$

Only three degrees-of-freedom were controlled initially, but the system is designed and is being developed for full control of at least 5 and possibly 6 degrees of freedom (Ref. 18).

A summary of digital controllers for MSBS wind tunnels is shown in table 2.

Table 2. Digital controllers for MSBS wind tunnels.

| Organization | Date | Degrees of Freedom | Controller Type |
|---|---|---|---|
| Oxford University | 1971 | 3 | phase-advance |
| MIT | 1976 | 1 | phase-advance |
| University of Southampton | 1981/84 | 2/6 | phase-advance |
| NASA Langley | 1984 | 5 | phase-advance |
| NAL | 1987/89 | 3/5 or 6 | proportion-integral-derivative |

### 4.2 Other Digitally Controlled Magnetic Suspension Systems

The first magnetic suspension system was originally developed for use as friction-free bearing for ultracentrifuge studies. Magnetic suspension systems are now being developed for transportation, magnetic bearings, and similar uses. It is worthwhile to review briefly the development of digital controllers for these uses since many of the problems and potential advantages are similar to those related to the use of digital control for MSBS used with wind tunnels.

#### 4.2.1 Loughborough, England:

A single degree-of-freedom demonstration system has been developed at Loughborough University, England (Ref. 19). The digital controller algorithm approximates the output and input as quadratic curves, shown in figure 11. The controller is located in the forward path of

the circuit. The coefficients of these quadratic curves can then be solved if three points along the curve are known; the present, and two previous values. The quadratic curves are:

$$\text{input:} \qquad \epsilon(t) = p + qt + rt^2 \tag{4.5}$$

$$\text{output:} \qquad V(t) = P + Qt + Rt^2$$

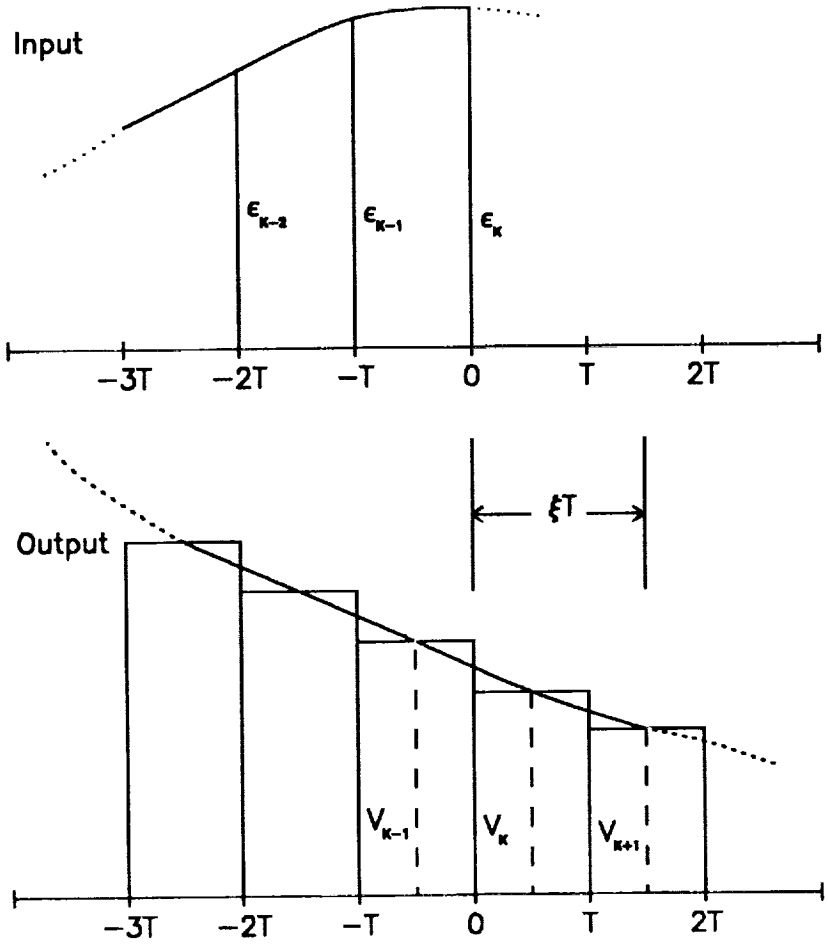


Figure 11. Sample timing for quadratic curve algorithm.

The coefficients of these quadratic curves can be solved in terms of the three points along the curves. The coefficients are:

$$p = \epsilon_k \qquad P = \frac{V_{k+1}\left(\zeta^2 - 3\zeta + 2\right) - 2\,V_k(\zeta^2 - 2\zeta) + V_{k-1}\left(\zeta^2 - \zeta\right)}{2}$$

$$q = \frac{(3\epsilon_k - 4\epsilon_{k-1} + \epsilon_{k-2})}{2T} \qquad Q = \frac{V_{k+1}\left(3 - 2\zeta\right) - 4\,V_k(1 - \zeta) + V_{k-1}(1 - 2\zeta)}{2T} \tag{4.6}$$

$$r = \frac{(\epsilon_k - 2\epsilon_{k-1} + \epsilon_{k-2})}{2T^2} \qquad R = \frac{(V_{k+1} - 2\,V_k + V_{k-1})}{2T^2}$$

To obtain the required control, the output $V_{k+1}$ of the controller is shifted forward an incremental time, $\zeta$. This shift forward in time is called *strike time* and is designed to overcome calculation and system time lags. The controller provides a control command for a point in the near future. With these quadratic equations and an appropriate time shift forward for the output, the algorithm can represent several different controllers. The algorithm has the form:

$$V_{k+1} = a_0\epsilon_k + a_{-1}\epsilon_{k-1} + a_{-2}\epsilon_{k-2} + b_0V_k + b_{-1}V_{k-1} \tag{4.7}$$

In equation 4.7 the coefficients are based on the quadratic curve fit coefficients obtained from equation 4.6 and the type of constants desired in the controller. If a dual phase-advance has the form $\frac{V}{\epsilon} = \left(\frac{1+nA\,S}{1+A\,S}\right)^2$, then the coefficients of equation 4.7 are:

$$a_0 = \left(1 + \frac{3\zeta}{2} + \frac{3nA}{T} + \frac{\zeta^2}{2} + \frac{2nA\zeta}{T} + \frac{\zeta^2}{T^2}\right)/\left(1 + \frac{3A}{T} + \frac{A^2}{T^2}\right)$$

$$a_{-1} = \left(-2\zeta - \frac{4nA}{T} - \zeta^2 - \frac{4nA\zeta}{T} - \frac{2n^2A^2}{T^2}\right)/\left(1 + \frac{3A}{T} + \frac{A^2}{T^2}\right)$$

$$a_{-2} = \left(\frac{\zeta}{2} + \frac{nA}{T} + \frac{\zeta^2}{2} + \frac{2nA\zeta}{T} + \frac{n^2A^2}{T^2}\right)/\left(1 + \frac{3A}{T} + \frac{A^2}{T^2}\right)$$

$$b_0 = \left(\frac{4A}{T} + \frac{2A^2}{T^2}\right)/\left(1 + \frac{3A}{T} + \frac{A^2}{T^2}\right)$$

$$b_{-1} = \left(\frac{-A}{T} - \frac{A^2}{T^2}\right)/\left(1 + \frac{3A}{T} + \frac{A^2}{T^2}\right)$$

### 4.2.2 Mitsui Engineering and Shipbuilding, Japan:

For many years, researchers in Japan have studied the use of magnetic suspension for high-speed trains. The first known use of digital control techniques was with a magnetically suspended linear guide developed in 1984 by Nippon Telegraph and Telephone, Kanagawa, as a technology demonstration (Ref. 20). Although the rate signals were derived from analog differentiators, the remainder of the control loop, including calculation of a coupling matrix, were carried out digitally. It appears that the digital hardware was custom built.

A single degree-of-freedom magnetic bearing has been digitally controlled using a microcomputer by Mitsui Engineering and Shipbuilding, Okayama. Three approaches to the synthesis of the digital controller were tested (Ref. 21).

The first approach used a digital simulation of a P I D controller. The digital controller uses the present and two previous position errors to determine the output command to the system. The rate prediction comes from a quadratic fit to the position error data. The values used for the proportional and derivative of the position error are at time 1.5T.

$$\frac{V}{\epsilon} = K\left[K_p + K_d\, S + \frac{K_{in}}{S}\right]$$

Using a quadratic fit to the position error data as in the Loughborough system:

$$\epsilon(t) = p + q\,t + r\,t^2$$

the position error and its derivative are calculated at time 1.5T.

$$\epsilon(1.5T) = p + q\,(1.5T) + r\,(1.5T)^2 \qquad \dot{\epsilon}(1.5T) = q + 2\,r\,(1.5T)^2$$

Also assuming the integral term is the sum of the position error data over time, the P I D controller is:

$$V_k = K\left[\left(\frac{15K_p}{8} + \frac{2K_d}{T}\right)\epsilon_{k-2} - \left(\frac{42K_p}{8} + \frac{5K_d}{T}\right)\epsilon_{k-1} + \left(\frac{35K_p}{8} + \frac{3K_d}{T}\right)\epsilon_k + K_{in}T\sum_{j=1}^{k}(\epsilon_j)\right] \tag{4.8}$$

A second controller uses a P D controller using the same system as in equation 4.8 and letting the integral gain, $K_{in} = 0$.

$$V_k = K\left[\left(\frac{15\,K_p}{8} + \frac{2\,K_d}{T}\right)\epsilon_{k-2} - \left(\frac{42\,K_p}{8} + \frac{5\,K_d}{T}\right)\epsilon_{k-1} + \left(\frac{35\,K_p}{8} + \frac{3\,K_d}{T}\right)\epsilon_k\right] \tag{4.8a}$$

The third method is a *z*-transformation of the P I D analog controller; where the P I D is represented as:

$$\frac{V}{\epsilon} = K\left[K_p + K_d\,S + \frac{K_{in}}{S}\right] = K\left[\frac{K_p\,S + K_d\,S^2 + K_{in}}{S}\right]$$

Using a four-point central difference approximation for the derivatives of $\epsilon$, then: (Ref. 22)

$$\dot{\epsilon} = \frac{\epsilon_{k-2} - 8\,\epsilon_{k-1} + 8\,\epsilon_{k+1} - \epsilon_{k+2}}{12\,T} \qquad \ddot{\epsilon} = \frac{-\epsilon_{k-2} + 16\,\epsilon_{k-1} - 30\,\epsilon_k + 16\,\epsilon_{k+1} - \epsilon_{k+2}}{12\,T^2}$$

The first derivative of V is approximated by backward-difference where:

$$\dot{V} = \frac{V_k - V_{k-1}}{T}$$

The P I D controller has the general form:

$$\frac{V}{\epsilon} = \frac{a_2 z^2 + a_1 z + a_0 + a_{-1} z^{-1} + a_{-2} z^{-2}}{1 - z^{-1}}$$

where: $a_2 = -\frac{K_p}{12} - \frac{K_d}{12\,T}$ $\qquad a_1 = \frac{8\,K_p}{12} + \frac{16\,K_d}{12\,T}$

$$a_0 = T\,K_{in} - \frac{30\,K_d}{12\,T}$$

$$a_{-1} = -\frac{8\,K_p}{12} + \frac{16\,K_d}{12\,T} \qquad a_{-2} = \frac{K_p}{12} - \frac{K_d}{12\,T}$$

This is presented as a difference equation:

$$V_k = a_2\,\epsilon_{k+2} + a_1\,\epsilon_{k+1} + a_0\,\epsilon_k + a_{-1}\,\epsilon_{k-1} + a_{-2}\,\epsilon_{k-2} + V_{k-1} \tag{4.9}$$

The values of $\epsilon_{k+1}$ and $\epsilon_{k+2}$ are calculated by using the quadratic approximation of the position error as used in equation 4.5.

$$\epsilon_{k+2} = 6\,\epsilon_k - 8\,\epsilon_{k-1} + 3\,\epsilon_{k-2} \qquad \epsilon_{k+1} = 3\,\epsilon_k - 3\,\epsilon_{k-1} + \epsilon_{k-2}$$

When these values are substituted back into equation 4.9, the output $V_k$ is expressed in terms of the inputs, $\epsilon_k$, $\epsilon_{k-1}$, and $\epsilon_{k-2}$.

$$V_k = (6a_2+3a_1+a_0)\,\epsilon_k + (-8a_2-3a_1+a_{-1})\,\epsilon_{k-1} + (3a_2+a_1+a_{-2})\,\epsilon_{k-2} + V_{k-1} \tag{4.10}$$

The next simplification is to let the initial value of the controller output, $V_0=0$, then for k=1,2,3,4,...

$$V_1= (6a_2+3a_1+a_0)\ \epsilon_1+ (-8a_2-3a_1+a_{-1})\ \epsilon_0+ (3a_2+a_1+a_{-2})\ \epsilon_{-1}$$

$$V_2= (6a_2+3a_1+a_0)\ \epsilon_2+ (-8a_2-3a_1+a_{-1})\ \epsilon_1+ (3a_2+a_1+a_{-2})\ \epsilon_0+ V_1$$

$$V_3= (6a_2+3a_1+a_0)\ \epsilon_3+ (-8a_2-3a_1+a_{-1})\ \epsilon_2+ (3a_2+a_1+a_{-2})\ \epsilon_1+ V_2$$

$$V_4= (6a_2+3a_1+a_0)\ \epsilon_4+ (-8a_2-3a_1+a_{-1})\ \epsilon_3+ (3a_2+a_1+a_{-2})\ \epsilon_2+ V_3$$

. . .

The equations above can then be rewritten as:

$$V_k= (5a_2+ 2a_1 - a_{-1}- a_{-2})\ \epsilon_k - (3a_2+a_1+a_{-2})\ \epsilon_{k-1}+ (a_2+a_1+a_0+a_{-1}+a_{-2}) \sum_{j=0}^{k} \epsilon_j \qquad (4.11)$$

This is a P I D digital controller using only two position-error data points.

### 4.2.3 Oak Ridge Gaseous Diffusion Plant, United States:

The Oak Ridge gaseous diffusion plant in cooperation with the University of Virginia developed a digital magnetic bearing system (Ref. 23). The fundamental approach of the controller is to generate an estimate of the derivative of the suspended object by real-time curve fitting of the position data. This single degree-of-freedom controller uses a polynomial least squares fit with exponential weighting to estimate the derivative in a P I D controller. The idea of using exponential weighting is that the data furthest back in time from the present should have the least effect on the output. The form of the P I D control algorithm is:

$$\frac{V}{\epsilon} = K\left[K_p + K_d\, S + \frac{K_{in}}{S}\right]$$

This controller assumes that the input to the controller is a polynomial curve of order n.

$$\epsilon(t) = a_0 + a_1 t + a_2 t^2 + a_3 t^3 + \ldots + a_n t^n \tag{4.12}$$

The coefficients of this polynomial are found by a least squares 'best fit' with a weighting factor. These coefficients of the polynomial are changed by incremental amounts, $\delta a_i$. The incremental changes $\delta a_i$ are determined by the order of the polynomial and the value of the weighting function, W, and remain constant. The calculated values for $\delta a_i$ are:

for (n=1) $\delta a_0 = 1 - W^2$ $\delta a_1 = (1 - W)^2$

for (n=2) $\delta a_0 = 1 - W^3$ $\delta a_1 = \frac{3}{2}(1 - W)^2(1 + W)$

$\delta a_2 = \frac{1}{2}(1 - W)^2$

for (n=3) $\delta a_0 = 1 - W^4$ $\delta a_1 = \frac{1}{6}(1 - W)^2(11 + 14W + 11W^2)$

$\delta a_2 = (1 - W)^3(1 + W)$ $\delta a_3 = \frac{1}{6}(1 - W)^4$

These incremental changes can be calculated for an $n^{th}$ order system.

The algorithm is used in two forms. One calculates a present time output and the other calculates a predicted time output.

For the present time output the controller algorithm is:

a) Decide the polynomial order, n and the weighting factor, W

b) Calculate the incremental changes in the polynomial coefficients, $\delta a_i$

c) Calculate present position error, $\epsilon_k = r - x_k$

d) Calculate the change in the errors from predicted, $\Delta\epsilon = \epsilon_k - a_0$

e) Sum up position error for integral term, $\sum\epsilon = \epsilon_k + \sum\epsilon$

f) Apply incremental change to coefficients, $a_i = a_i + \delta a_i \Delta\epsilon$ where i=0 to n

g) Calculate present control output,

$$V = K\left[K_p\epsilon_k + K_{d_1}a_1 + 2\,K_{d_2}a_2 + K_{in}\sum\epsilon\right] \tag{4.13}$$

h) Return to c)

The predicted time output calculates the output from the controller at one time step forward using the present coefficients and shifting them forward. This is accomplished by substituting t=t+T into equation 4.12, where T is one time unit. Then:

$$\epsilon'(t) = a_0 + a_1(t+T) + a_2(t+T)^2 + a_3(t+T)^3 + \ldots + a_n(t+T)^n$$

Collecting the coefficients the predicted polynomial is:

$$\epsilon'(t) = a'_0 + a'_1 t + a'_2 t^2 + \ldots + a'_n t^n \tag{4.14}$$

where:

$$a'_0 = a_0 + a_1 + a_2 + a_3 + a_4 + \ldots$$

$$a'_1 = a_1 + 2a_2 + 3a_3 + 4a_4 + \ldots$$

$$a'_2 = a_2 + 3a_3 + 6a_4 + \ldots$$

$$a'_3 = a_3 + 4a_4 + \ldots$$

$$\ldots$$

$$a'_n = a_n$$

The predicted time output algorithm is:

a) Decide the polynomial order, n and the weighting factor, W

b) Calculate the incremental changes in the polynomial coefficients, $\delta a_i$

c) Calculate present position error, $\epsilon_k = r - x_k$

d) Calculate the change in the errors form predicted, $\Delta\epsilon = \epsilon_k - a'_0$

e) Sum up position error for integral term, $\sum\epsilon = \epsilon_k + \sum\epsilon$

f) Apply incremental change to coefficients, $a_i = a_i + \delta a_i \Delta\epsilon$ where i=0 to n

g) Shift the polynomial coefficients forward one time set.

h) Calculate the predicted control output,

$$V = K\left[K_{p_+}a'_0 + K_p a_0 + K_{d_{+1}}a'_1 + 2K_{d_{+2}}a'_2 + K_{d_1}a_1 + 2K_{d_2}a_2 + K_{in}\sum\epsilon\right] \quad (4.15)$$

i) return to c)

These two controllers allow the operator to select any order polynomial and any weighting factor for the control algorithm. The controller is located in the forward path. This system provides the most involved controller of all those discussed.

### 4.2.4 UVa Electrical Engineering, United States:

Magnetic suspensions are used at two locations at the University of Virginia and digital controllers are being developed for use with these systems.

One group is the Electrical Engineering Department which is studying the use of magnetic bearings for a rotating shaft (Ref. 24). The system digitally controls the magnetic bearing through a microcomputer using assembly language. The magnetic bearing system uses a digital P D controller located in the feedback path where $S = \frac{(z-1)}{T z}$. The general form of a P D controller is:

$$\frac{V}{\epsilon} = \left[K_p + K_d S\right]$$

When the z-transform of the derivative is substituted into the general form, the equation is:

$$V_k = K_p\,\epsilon_k + \frac{K_d}{T}\left(\epsilon_k - \epsilon_{k-1}\right) \tag{4.16}$$

This digital controller in equation 4.16 is very simple and provides adequate control of the shaft with the magnetic bearings. The simplicity of this program allows very high computational speeds.

### 4.2.5 UVa Nuclear Engineering and Engineering Physics, United States:

The other group at UVa is in the Department of Nuclear Engineering and Engineering Physics. Magnetic suspension is used in this department for experimental studies of gravitation and general relativity (Ref. 25). The controller is a digital P I D located in the forward path and analog filters. The digital P I D is of the form:

$$V = K\left[K_p\epsilon + K_d\dot{\epsilon} + K_{in}\int \epsilon\, dt\right]$$

where the derivative is calculated using the first two terms of a Taylor series, where:

$$\dot{\epsilon} = \frac{\epsilon_k - \epsilon_{k-1}}{T}$$

The integral term is derived by using the Trapezoidal Rule, where:

$$\int_{k-1}^{k} \epsilon\, dt \simeq \frac{T}{2}\left(\epsilon_k + \epsilon_{k-1}\right)$$

This integral value is then summed up over the entire time.

$$\sum\epsilon = \sum\epsilon + \frac{T}{2}\left(\epsilon_k + \epsilon_{k-1}\right)$$

The proportional, derivative, and integral terms are then added to obtain the controller output.

$$V = K\left[\left(K_p + \frac{K_d}{T}\right)\epsilon_k - \frac{K_d}{T}\epsilon_{k-1} + K_{in}\sum\epsilon\right] \tag{4.17}$$

This digital controller is simple and provides adequate control of a suspended sphere.

A summary of digital controllers for magnetic suspension systems is shown in table 3.

Table 3. Digital controllers for magnetic suspension systems.

| Organization | Date | Controller Type | Method |
|---|---|---|---|
| Loughborough University | 1986 | phase-advance | quadratic fit |
| Mitsui Engineering and Shipbuilding | 1984 | P I D and P D | quadratic fit difference equation |
| Oak Ridge Gaseous Diffusion Plant | 1986 | P I D | exponential weighting with polynominal fit |
| University of Virginia, Dept. of Electrical Engineering | 1987 | P D | $z$-transformation |
| University of Virginia Dept. of Nuclear Engineering and Engineering Physics | 1989 | P I D | difference equation |

# 5. DIGITAL SIMULATION

## 5.1 Derivation of Equations for Simulation

The MSBS plant described by equation 2.10 is for a single degree-of-freedom MSBS. This plant can be discretized by several different methods. One method is the Tustin's transformation which is only an approximation of a conversion between the *S*-domain and the *z*-domain (Ref. 26). For the Tustin's transformation:

$S = \frac{2}{T}\frac{(z-1)}{(z+1)}$, where T is the sampling time.

As given in equation 2.10b the MSBS plant is:

$$\Delta X = \frac{-\frac{K_i}{m L}\Delta V + \frac{R}{m L}\left(1+\frac{L}{R}S\right) f}{S^3 + S^2\left(\frac{R}{L}+\frac{C}{m}\right) + S\left(\frac{C R}{m L} - \frac{K_x}{m} - \frac{K_i K_c}{L m}\right) - \frac{R K_x}{L m}}$$

For zero input force disturbance, (f=0), the Tustin's transformation of this equation is:

$$\frac{\Delta X}{\Delta V} = \frac{a_0[1+ z^{-1}+ z^{-2}+ z^{-3}]}{b_0 + b_1 z^{-1} + b_2 z^{-2} + b_3 z^{-3}} \qquad (5.1)$$

where $a_0 = \frac{-K_i}{m L}$

$$b_0 = \left(\frac{2}{T}\right)^3 + \left(\frac{2}{T}\right)^2\left(\frac{R}{L}+\frac{C}{m}\right) + \frac{2}{T}\left(\frac{C R}{m L} - \frac{K_x}{m} - \frac{K_i K_c}{L m}\right) - \frac{R K_x}{L m}$$

$$b_1 = -3\left(\frac{2}{T}\right)^3 - \left(\frac{2}{T}\right)^2\left(\frac{R}{L}+\frac{C}{m}\right) + \frac{2}{T}\left(\frac{C\,R}{m\,L} - \frac{K_x}{m} - \frac{K_i\,K_c}{L\,m}\right) - 3\,\frac{R\,K_x}{L\,m}$$

$$b_2 = 3\left(\frac{2}{T}\right)^3 - \left(\frac{2}{T}\right)^2\left(\frac{R}{L}+\frac{C}{m}\right) - \frac{2}{T}\left(\frac{C\,R}{m\,L} - \frac{K_x}{m} - \frac{K_i\,K_c}{L\,m}\right) - 3\,\frac{R\,K_x}{L\,m}$$

$$b_3 = -\left(\frac{2}{T}\right)^3 + \left(\frac{2}{T}\right)^2\left(\frac{R}{L}+\frac{C}{m}\right) - \frac{2}{T}\left(\frac{C\,R}{m\,L} - \frac{K_x}{m} - \frac{K_i\,K_c}{L\,m}\right) - \frac{R\,K_x}{L\,m}$$

For the case when $f \neq 0$ the Tustin's transformed MSBS plant is:

$$\Delta X = \frac{a_0[1+ z^{-1}+ z^{-2}+ z^{-3}]\Delta V + [a_1+ a_2 z^{-1}+ a_3 z^{-2}+ a_4 z^{-3}]\,f}{b_0 + b_1\, z^{-1} + b_2\, z^{-2} + b_3\, z^{-3}} \qquad (5.2)$$

where the additional coefficients are:

$$a_1 = \left(\frac{R}{m\,L} + \frac{2}{mT}\right) \qquad a_2 = \left(\frac{3\,R}{m\,L} + \frac{2}{mT}\right)$$

$$a_3 = \left(\frac{3\,R}{m\,L} - \frac{2}{mT}\right) \qquad a_4 = \left(\frac{R}{m\,L} - \frac{2}{mT}\right)$$

Using equation 5.2 as the discretized MSBS plant, a simulation can be designed for use on a microcomputer. This simulation will allow design work for development and comparison of control algorithms.

## 5.2 Simulation Program

The simulation program is written in the BASIC language (Ref. 27). As with most microcomputer languages, BASIC allows great flexibility in the type of control algorithms that can be implemented on microcomputers for use as MSBS controllers. Because most MSBS systems use microcomputers to control the system, the BASIC language program can be used on an MSBS system or transformed to another computer language for use.

The simulation program includes the digital controllers discussed in chapter 4. The simulation allows the parameters of the MSBS plant to be changed easily and to observe the effects these variations have on the system performance. Also, the simulation program has the ability to vary the parameters in the controller and the type or method of control used for the MSBS. The program allows two types of step inputs to the system, a position input and a force input.

A standard simulation run starts with a unit step position input at simulation time t=0. At simulation time t=5 seconds a 10-unit step force input is commanded. The simulation run then stops at t=20 seconds. The program has a graphical display of the suspended body position trajectory. This graphical display can be scaled to provide a detailed view of the trajectory. The program also calculates and displays, above the trajectories, certain design parameters that can be used to compare systems' performances. These design parameters are gains, rise time, peak times, settling times, overshoots, time, and position. The complete listing of the program is given in Appendix A.

## 5.3 Representative Magnetic Suspension and Balance System

The choice of a representative MSBS plant for use in the simulation program is critical in order to determine how different controllers perform. This representative MSBS should exhibit the same dynamic characteristics as a real plant. These characteristics are determined by the location of the poles. As shown in equation 2.10, the pole locations are influenced by many parameters of the system. Many technical papers have addressed the problem of plant model verification with experimental results. The model described in equation 2.10 is more complex than most linearized models. Comparisons between experimental results and linearized models show that the dynamics of a magnetic suspension system are accurately described.

To obtain the desired MSBS plant dynamics, three poles are needed with locations similar to those shown in figure 6. Based on the relative location of the poles for a real MSBS plant, a

suitable choice for the poles of our representative MSBS are: $P_1 \simeq -10$, $P_2 \simeq -1$, and $P_3 \simeq 1$. To realize these poles, the parameters of the system, as described in equation 2.10, are:

$R = 1$ $\quad L = 0.1$ $\quad K_x = 1$

$K_i = 0.1$ $\quad K_c = -0.1$ $\quad m = 1$

$C = 0$

With these parameters the actual pole locations of the representative MSBS are $P_1 = -9.9899$, $P_2 = -1.0056$, and $P_3 = 0.9955$. The plant transfer function therefore is:

$$\Delta X = \frac{-\Delta V + 10\left(1 + 0.1\,S\right) f}{S^3 + 10\,S^2 - 0.9\,S - 10} \tag{5.3}$$

The actual choice of pole locations for this representative plant are not completely random. Recent work at the NASA Langley 13-inch MSBS has been toward developing a mathematical model of the system. The early results show the actual system has pole locations similar to those chosen for the representative plant. Also several reports have shown that the linear approximations give a good representation of the MSBS dynamics (Ref. 4).

# 6. COMPARISON OF CONTROLLERS BY SIMULATION PROGRAM

The simulation program can be easily used to compare the responses of different control algorithms on a representative MSBS plant. As shown in chapter 4, there are several philosophies of how a digital controller is derived and the type of controller. Each method has advantages and disadvantages with the final decision based on the desired system performance.

Studying digital controller algorithms is best carried out with a computer simulation program. Standard control systems analysis will not show the difference caused when deriving a digital controller. These differences are brought about because of approximations made when converting an analog controller to a digital controller. With the simulation program, the exact method of how the controller is executed can be programmed. The simulation allows the method of control to be changed or modified for comparison and development. The main purpose of the simulation is to study the different controllers to determine the advantages and disadvantages of a particular control system and compare several of their performance characteristics.

## 6.1 Location of Controller

The two primary uses for magnetic suspension systems are for large gap suspension and small gap suspension. The difference between large or small gap is based on the distance between the electromagnets and the suspended body.

Large gap systems include those associated with wind tunnels. These systems require position input commands to change model position and orientation during wind tunnel tests. The wind tunnel system must also maintain position and orientation when loads are being

applied to the model. On the other hand, magnetic bearing suspension systems are small gap systems. Due to the small gaps, they seldom require a position input command, being mainly required to maintain a fixed position under applied loads.

The large and small gap systems also have a difference in the power requirements. The current used in maintaining the suspension is several times greater in a large gap system than a small gap system. For example the NASA 13 inch MSBS requires approximately 20 amps in each coil to suspend a model; whereas, the Loughborough MSBS and other magnetic bearing systems use less than 1 amp in the coil.

The different requirements and power levels for these two systems has produced two classes of controllers. Most wind tunnel suspension systems have used the phase advance controller located in the feedback path of the control circuit and an integral term located in the forward path. Typically these controllers have performed well to the position inputs and force inputs.

Most magnetic bearing suspension systems use a P I D controller located in the forward path of the control circuit. This forward path P I D controller responds well to force inputs but poorly to step position inputs.

The poor performance of the forward path controller to a step position input is caused by the lead compensation located in the forward path. Given a step position input, the initial derivative term of the controller is very large which causes a large first overshoot. The large overshoot is not a problem for a bearing system because position inputs are not expected. The bearing shaft would only momentarily touch the wall of the bearing and would quickly recover and continue to function properly. This large overshoot can be avoided by not allowing step inputs to the controller but rather limit the commands to ramp inputs. An advantage of having the controller in the forward path is to provide a quick response when compared to controllers located in the feedback path.

An example of this large overshoot is shown in figure 12. The top graph is the position trajectory of a P I D controller with the P D part of the controller being located in the feedback

path. The lower graph is of the same P I D controller with the entire controller located in the forward path. Each of these controllers have identical gains and are subject to the standard simulation run. The only difference is the location of the P and D parts of the controller. These gains are based on a 5% overshoot performance for a position input of a P I D controller with the P D located in the feedback path.

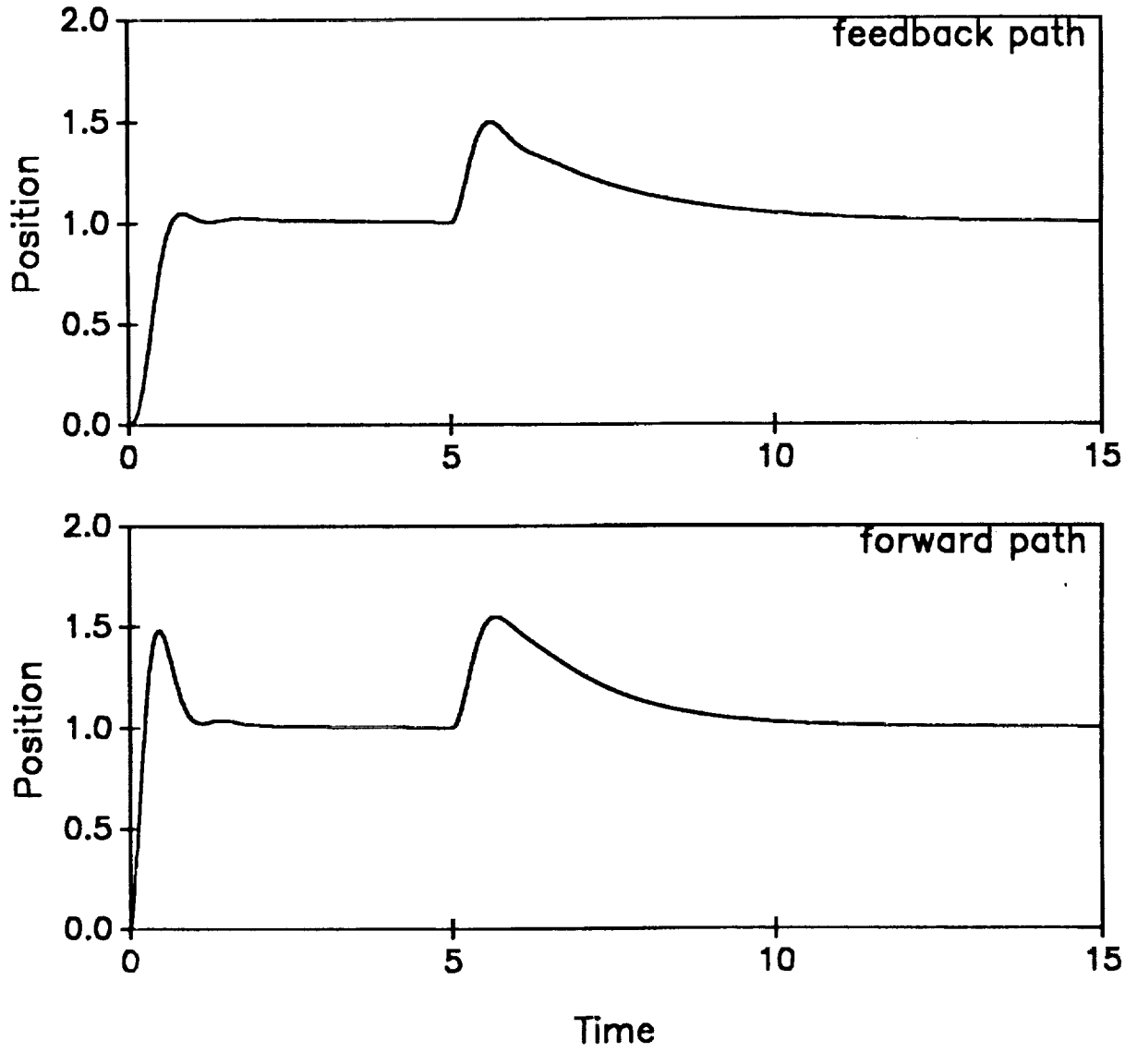


Figure 12. Position trajectories of P I D, (controller location).

Figure 12 shows the large overshoot produced by a step position input to the forward path controller as compared with the feedback controller. The response to the force inputs are almost identical with only minor differences caused by the integral term. The results of these responses are shown in table 4. The extremely large overshoot of 48% for the forward path controller is unacceptable. It is possible to design the forward path P I D controller having a 5% overshoot to a step position input but the controller then does not have sufficient stiffness to withstand large force inputs. By adjusting the overall gain of the forward path P I D controller, a minimum first overshoot can be found. In table 4 the P I D "best" is the best response to a unit step position input for the forward path P I D controller.

Table 4. P I D controller location. (Position input)

| Controller | Overall Gain | Rise Time, s | Peak Time, s | Settling Time, s | First Overshoot |
|---|---|---|---|---|---|
| P I D, feedback | 362 | 0.41 | 0.84 | 1.29 | 1.050 |
| P I D, forward | 362 | 0.17 | 0.46 | 1.15 | 1.481 |
| P I D, "best" | 522 | 0.13 | 0.35 | 1.64 | 1.470 |

This large overshoot is also present when using a dual phase-advance controller in the forward path. Figure 13 shows two position trajectories for dual phase-advance controllers. The top trajectory is for the controller located in the feedback path and in the bottom trajectory the controller is located in the forward path. Each controller is subject to a standard simulation run.

Again the forward path has an unacceptable first overshoot. These dual phase advance controllers are identical except for the location of the controller. The gains are based on a 5% overshoot performance for the feedback dual phase-advance controller. The results of these responses for a step position input are shown in table 5. The responses to the force input are nearly identical.

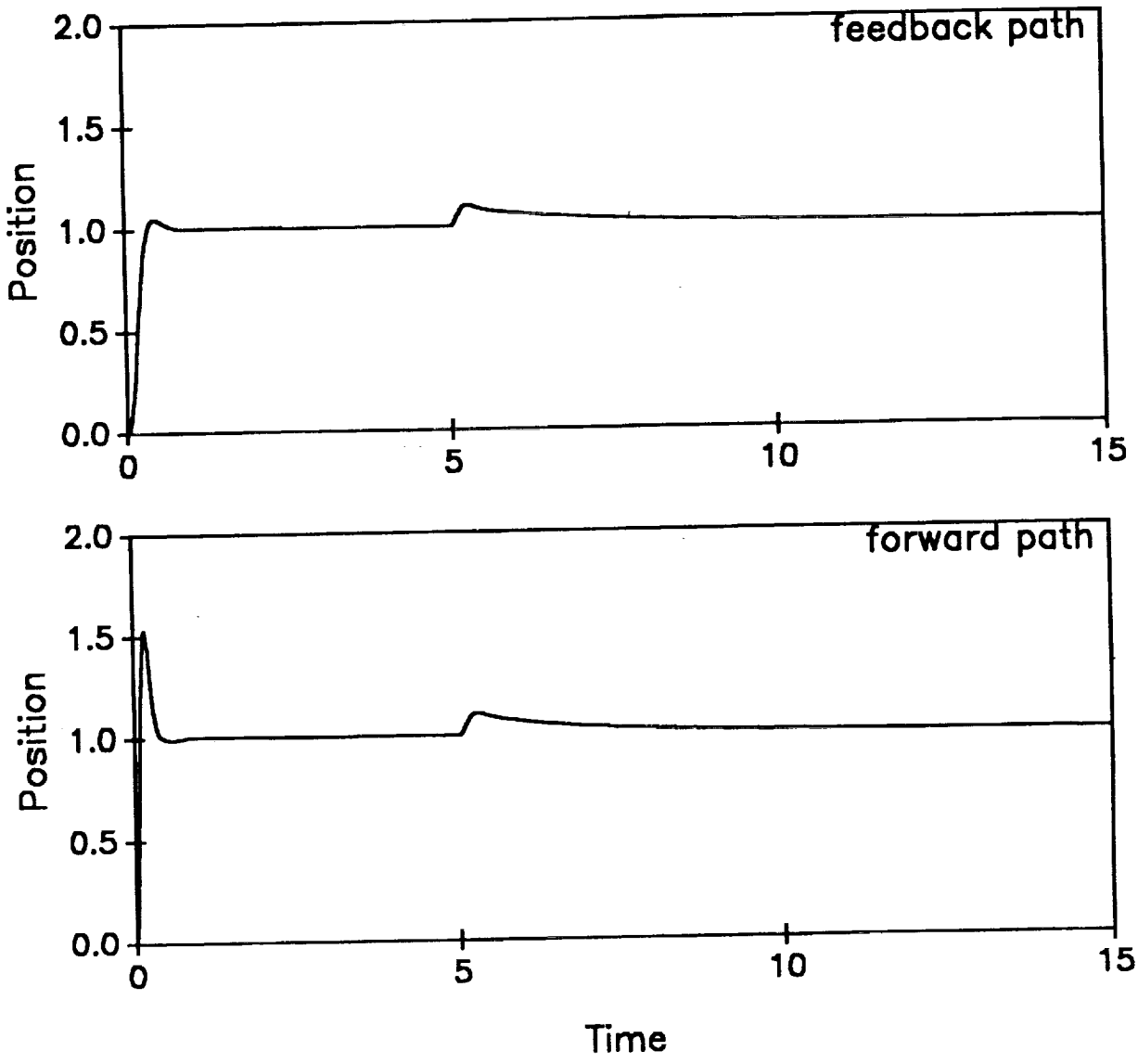


Figure 13. Position trajectories of D P A, (controller location).

Table 5. D P A controller location. (Position input)

| Controller | Overall Gain | Rise Time, s | Peak Time, s | Settling Time, s | First Overshoot |
|---|---|---|---|---|---|
| D P A, feedback | 2080 | 0.21 | 0.47 | 0.93 | 1.050 |
| D P A, forward | 2080 | 0.07 | 0.18 | 0.63 | 1.528 |
| D P A, "best" | 1602 | 0.08 | 0.22 | 1.05 | 1.487 |

By adjusting the overall gain of the forward path dual phase-advance controller, a minimum first overshoot can be found. In table 5, the dual phase advance "best" has the best response to a unit step input for the forward path controller.

The rise, peak, and settling times are greatly improved by having the controller located in the forward path. However, these advantages are overshadowed by the unacceptable first overshoot.

Using a controller in the forward path of a wind tunnel system could be dangerous. During a large overshoot the model could be lost from the view of the position sensors causing loss of model control. This is not to say that forward path controllers should never be used. However, care should be taken in the type of position inputs given to the controller.

## 6.2 Comparison of Dual Phase Advance Controllers

To compare the different algorithms of the digital phase-advance controllers, the constants within the controllers must be the same. Each dual phase-advance controller is located in the feedback path and has an integrator added to the forward path to help improve performance by driving the steady-state error to zero. This integrator is based on equation 4.3. The integral gain is set at $K_{in}$=0.5 in all the algorithms. The controller time constant is also fixed at A=0.01. The high/low frequency gain is set to n=10. The only adjustable constant in each controller is the overall gain, K. With the constants being the same in each controller, the differences in performance of the digital dual phase-advance controllers can be compared.

There are four dual phase-advance controllers that are compared using the simulation program. These are the Tustin's D P A, Southampton, NASA, and Loughborough controllers. For the Tustin's D P A algorithm, the Tustin's method is used to discretize a dual phase-advance controller. The derivation of the Tustin's D P A controller is shown in Appendix B as equation B-3. The Southampton controller is obtained from equations 4.2a and 4.2b, the NASA controller is from equations 4.4a, 4.4b, and 4.4c, and the Loughborough controller is from equation 4.7.

Because the wind tunnel type controllers are concerned with position and force inputs, the performance analysis must include these inputs. A standard comparison run starts at the simulation time t=0 with a unit step position input. At simulation time t=5 seconds a 10 unit step force input is commanded. The computer program stops after 20 seconds of simulation time. The performance of the controller can be determined from these two input commands.

### 6.2.1 5% Overshoot Performance:

For dual phase-advance controllers, one design criterion for comparing the controllers is to adjust the overall gain for a first overshoot of 5% for a unit step position input. Figure 14 shows the position trajectories for this 5% position input overshoot of each controller.

The results of these trajectories are shown in tables 6(a) and 6(b). Table 6(a) shows several performance parameters obtained from a position input. Table 6(b) shows the performance parameters obtained from a force input.

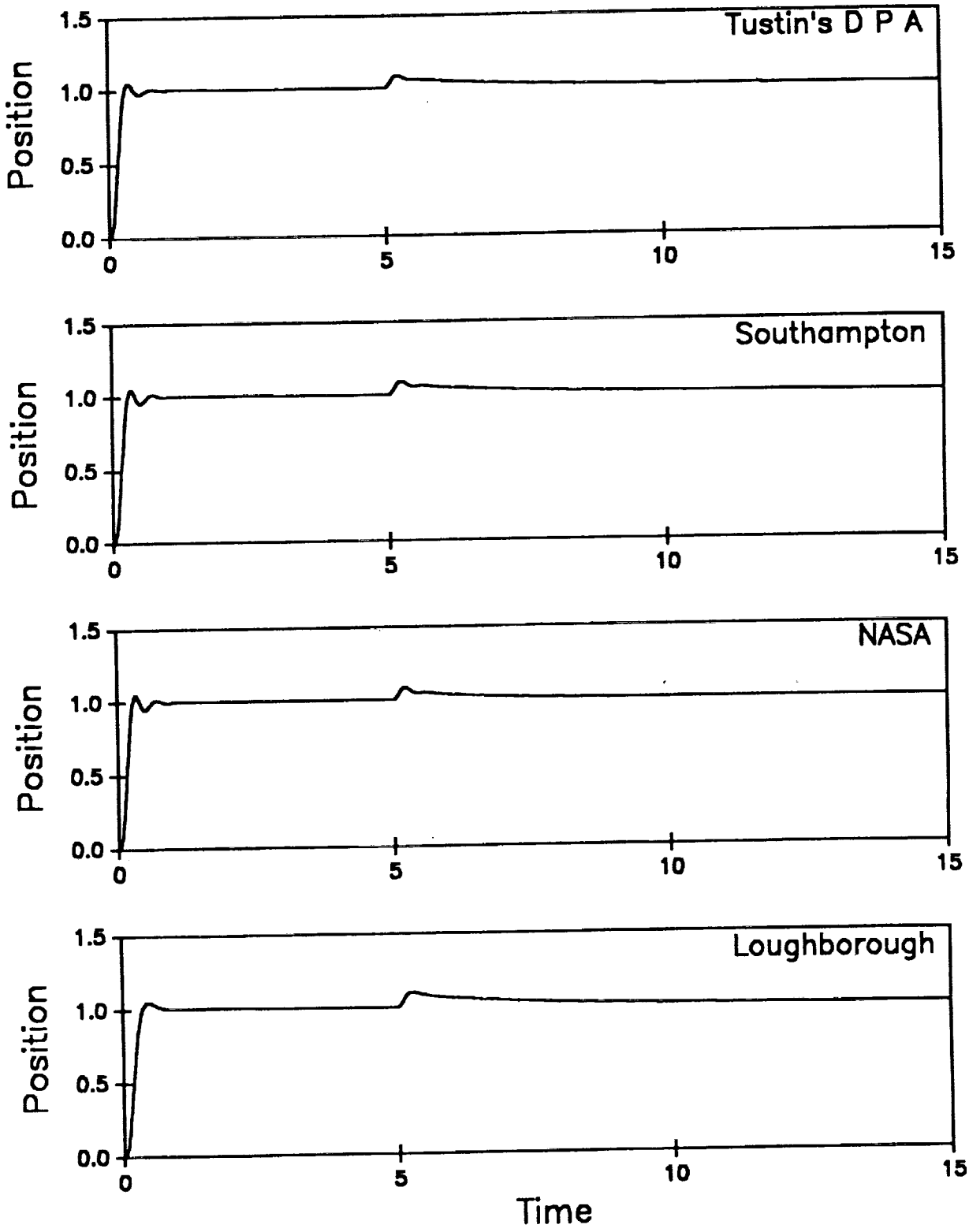


Figure 14. Position trajectories of D P A controllers, 5% overshoot.

Table 6(a). D P A, 5% overshoot. (Position input)

| Method of discretization | Overall Gain | Rise Time, s | Peak Time, s | Settling Time, s | First Overshoot |
|---|---|---|---|---|---|
| Tustin's D P A | 2784 | 0.18 | 0.36 | 0.83 | 1.050 |
| Southampton | 2665 | 0.17 | 0.34 | 0.96 | 1.050 |
| NASA | 2720 | 0.17 | 0.33 | 0.95 | 1.050 |
| Loughborough | 2080 | 0.21 | 0.47 | 0.93 | 1.050 |

Table 6(b). D P A, 5% overshoot. (Force input)

| Method of discretization | Overall Gain | Peak Time, s | Settling Time, s | Overshoot | Final Position |
|---|---|---|---|---|---|
| Tustin's D P A | 2784 | 0.24 | 15.00 | 1.083 | 1.00 |
| Southampton | 2665 | 0.23 | 15.29 | 1.090 | 1.00 |
| NASA | 2720 | 0.22 | 11.34 | 1.086 | 1.00 |
| Loughborough | 2080 | 0.27 | 15.77 | 1.102 | 1.00 |

These results show that all the controllers perform well in controlling the system with little difference in their performances. However the results for a position input show that the Tustin's D P A controller performs "best" because of its low settling time. The rise and peak times of the Tustin's D P A controller are similar to those of the NASA and Southampton controllers.

Table 6(b) shows the results from a force input. This is important because it shows the spring-like stiffness of the system which is caused by the controller. This stiffness is related to the overshoot caused by a force input. The Tustin's D P A and NASA controllers have nearly equal stiffness. Table 6(b) shows that the NASA method provides the "best" settling time from a force input to the controller.

The integral gain, $K_{in}$ has a major influence in the response to a force input. A high integral gain improves the response to force inputs by reducing the settling time. This high gain also increases instability.

### 6.2.2 Minimum First Overshoot Performance:

With increased overall gain for the dual phase-advance controller, the system response represents an overdamped system. The system performance is improved if the overall gain is increased so the first overshoot is minimum for a position input. Any increase in gain causes the second overshoot to be larger than the first overshoot. Figure 15 shows the position trajectories of each system based on this minimum first overshoot gain value.

Tables 7(a) and 7(b) show the different controllers' performances based on the minimum first overshoot system performance.

Table 7(a). D P A, minimum first overshoot. (Position input)

| Method of discretization | Overall Gain | Rise Time, s | Peak Time, s | Settling Time, s | First Overshoot |
|---|---|---|---|---|---|
| Tustin's D P A | 3202 | 0.18 | 0.35 | 0.76 | 1.005 |
| Southampton | 2939 | 0.17 | 0.33 | 0.88 | 1.014 |
| NASA | 2995 | 0.17 | 0.32 | 1.04 | 1.014 |
| Loughborough | 3115 | 0.26 | 0.54 | 0.59 | 1.013 |

Table 7(b). D P A, minimum first overshoot. (Force input)

| Method of discretization | Overall Gain | Peak Time, s | Settling Time, s | Overshoot | Final Position |
|---|---|---|---|---|---|
| Tustin's D P A | 3202 | 0.22 | 14.80 | 1.071 | 1.00 |
| Southampton | 2939 | 0.21 | 14.89 | 1.081 | 1.00 |
| NASA | 2995 | 0.21 | 11.21 | 1.077 | 1.00 |
| Loughborough | 3115 | 0.19 | 14.84 | 1.062 | 1.00 |

Tables 7(a) and 7(b) show that operating the system with minimum first overshoot improves the performance when compared to the 5% overshoot system shown in tables 6(a) and 6(b). The minimum first overshoot controllers have better rise, peak, and settling times plus an increase in the stiffness of the system.

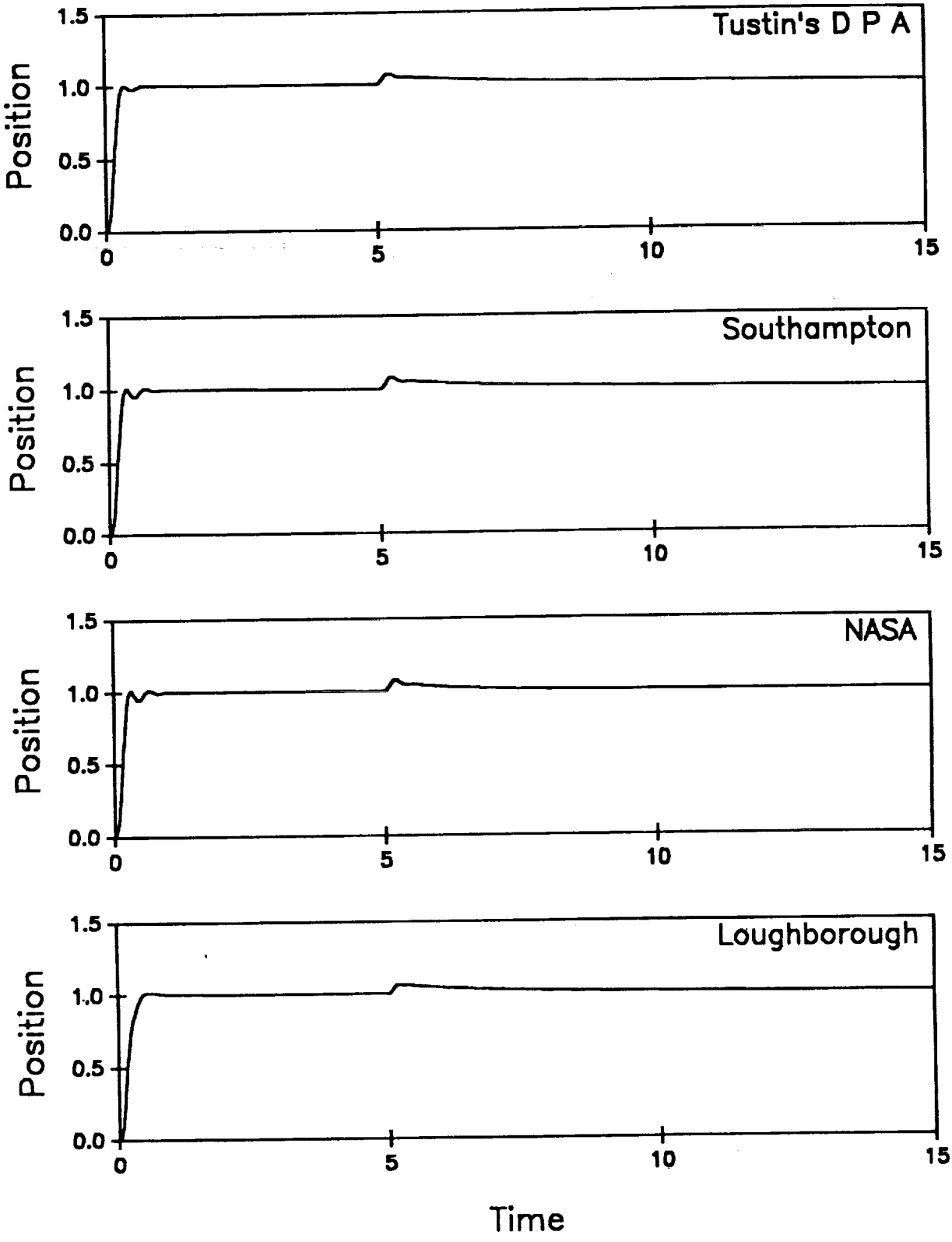


Figure 15. Position trajectories of D P A controllers, minimum first overshoot.

From table 7(a), using the settling time as the performance criteria, the Loughborough controller is the "best", except for its rise time and peak times. If choosing a controller based on the minimum first overshoot system performance, the Loughborough controller is preferred because of its low settling time.

In table 7(b) the response of a force input is given which shows that the Loughborough controller provides the "best" stiffness. The NASA controller provides the "best" settling time.

### 6.2.3 Execution Times:

One of the seldom mentioned design criteria for digital controllers for MSBS is execution time. Execution time is extremely important in providing a good controller. Execution time is based on the number of calculations each controller must make in order to operate. Execution time is highly dependent upon the hardware and software that the controller uses. The faster controllers having a short execution time are preferred if they can provide adequate control of the system. Table 8 shows a representative time required to complete 25000 cycles of the controllers using the simulation program. Each of these dual phase-advance controllers have nearly equal execution times. The best controllers in terms of execution time are the Tustin's and Loughborough controllers.

Table 8. D P A relative execution times.

| Method of discretization | Execution Time, s |
|---|---|
| Tustin's D P A | 40 |
| Southampton | 43 |
| NASA | 43 |
| Loughborough | 40 |

The difference in the "best" controllers for a 5% overshoot system and a minimum first overshoot system shows how important it is to choose a design criteria which best suits the desired system performance. Because there are many possible uses for the controllers, one should base the choice of controller on the expected use and desired performances of the system.

## 6.3 Comparison of Proportional Integral Derivative Controller

As shown earlier, controllers located in the forward path of an MSBS system have a large first overshoot to step-position input. Comparison of controllers in their forward path is useful even though they would perform better if located in the feedback path. Most of the P I D controllers used with magnetic bearing systems are located in the forward path. The comparison of the forward path controllers is useful because the response to force inputs and the stiffness of the system will be the same regardlesss of the controllers' location. These force responses and stiffness can then be compared with other controllers.

To compare the P I D controllers in the forward path, a set of design criteria must be established. To compare the P I D controllers, each controller must have the same gains within the controller and adjust only the overall gain of the controller. The constants chosen are $K_p$=1, $K_d$=0.4, and $K_{in}$=0.5. The value of the integral gain is the same as the value used in the phase advance controller comparison. The proportional and derivative gains were obtained from an analysis of the UVa controller described in equation 4.16. The proportional and derivative gains are based on the best possible response of this P I D controller. As shown earlier, a P I D controller in the forward path does not have an acceptable first overshoot response to a unit step position input.

There are six P I D controllers which are compared using the simulation program. These P I D controllers will be referred to as Tustin's P I D, equation 4.8, equation 4.10, equation 4.11, equation 4.16 and equation 4.17. The Tustin's P I D controller is derived in Appendix B as equation B-5. The controller described by equations 4.8, 4.10, and 4.11 are all derivations

from Mitsui Engineering and Shipbuilding. The fifth controller, equation 4.16, is from the UVa Electrical Engineering Department and equation 4.17 from the UVa Nuclear Engineering and Engineering Physics Department.

One controller described in chapter 4 that is not used in this comparison is the Oak Ridge controller described by equations 4.13 and 4.15. The described controller algorithm will not control the simulated MSBS plant. The published documentation of this control algorithm is thought to contain an error and further clarification is being sought (Ref. 23).

### 6.3.1 Minimum First Overshoot Performance:

The design criteria for comparing the P I D controllers are to minimize the first overshoot for a unit step-position input and to have the highest possible overall gain. In each case there is a unique gain which provides a minimum first overshoot.

The simulation run is the same as used with the dual phase advance controllers. At simulation time t=0 a unit step-position input is commanded. Following this at time t=5 seconds a step-force input of 10 units is given. The simulation stops after 20 seconds.

The resulting position trajectories for each controller are shown in figure 16. The performance characteristics of these P I D controllers are presented in tables 9(a) and 9(b).

Table 9(a). P I D, minimum first overshoot. (Position input)

| Method of discretization | Overall Gain | Rise Time, s | Peak Time, s | Settling Time, s | First Overshoot |
|---|---|---|---|---|---|
| Tustin's P I D | 396 | 0.16 | 0.43 | 1.38 | 1.569 |
| Equation 4.8 | 522 | 0.13 | 0.35 | 1.64 | 1.470 |
| Equation 4.10 | 359 | 0.17 | 0.46 | 1.45 | 1.594 |
| Equation 4.11 | 360 | 0.17 | 0.46 | 1.45 | 1.594 |
| Equation 4.16 | 361 | 0.17 | 0.46 | 2.02 | 1.598 |
| Equation 4.17 | 359 | 0.17 | 0.46 | 1.47 | 1.598 |

Table 9(b). P I D, minimum first overshoot. (Force input)

| Method of discretization | Overall Gain | Peak Time, s | Settling Time, s | Overshoot | Final Position |
|---|---|---|---|---|---|
| Tustin's P I D | 396 | 0.60 | 15.71 | 1.506 | 1.00 |
| Equation 4.8 | 522 | 0.55 | 15.02 | 1.346 | 1.00 |
| Equation 4.10 | 359 | 0.62 | 15.57 | 1.567 | 1.00 |
| Equation 4.11 | 360 | 0.62 | 15.43 | 1.565 | 1.00 |
| Equation 4.16 | 361 | 0.62 | 15.39 | 1.568 | 1.00 |
| Equation 4.17 | 359 | 0.63 | 15.47 | 1.573 | 1.00 |

From figure 16, and tables 9(a) and 9(b) the "best" P I D controller is described by equation 4.8. This controller has the fastest rise and peak times and the lowest overshoot for a position input. The Tustin's P I D has the "best" settling time. For a force input, the equation 4.8 controller has the largest stiffness as shown by the low overshoot value from a force input as shown in table 9(b). The equation 4.8 controller also has the "best" settling time from a force input.

The controllers of equations 4.10 and 4.11 are nearly identical in response because equation 4.11 is a derivation of equation 4.10. The method used in deriving the algorithm for equations 4.16 and 4.17 is simple and provides a similar response to the complex algorithms of equations 4.10 and 4.11.

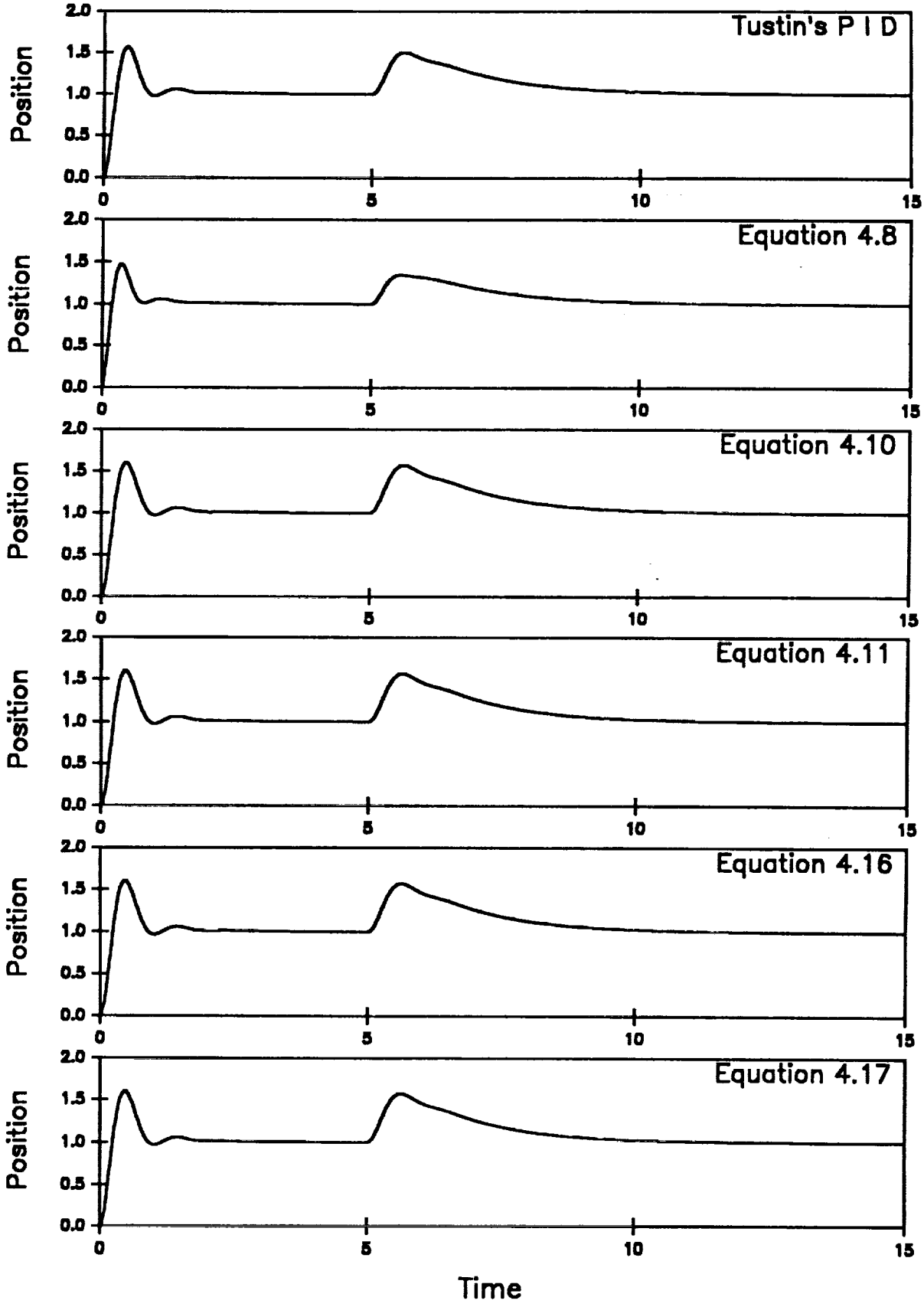


Figure 16. Position trajectories of P I D controllers, minimum first overshoot.

### 6.3.2 Execution Times:

The execution times for the P I D controllers were determined by the same method as used for the execution times of the dual phase advance controllers. Table 10 shows the execution time required to complete 25000 cycles of the controller. The table shows that each P I D has nearly identical execution times.

Table 10. P I D relative execution times.

| Method of discretization | Execution Time, s |
|---|---|
| Tustin's P I D | 35 |
| Equation 4.8 | 35 |
| Equation 4.10 | 34 |
| Equation 4.11 | 34 |
| Equation 4.16 | 35 |
| Equation 4.17 | 35 |

# 7. CONCLUSIONS AND RECOMMENDATIONS

## 7.1 Best Overall Controller

The choice of the "best" overall controller is completely dependent on the desired system performance and intended use. The best location for the controller is the feedback path. The advantages of a forward path controller in reducing the rise, peak, settling, and execution time, do not overcome the inability to adequately control the system for a step-position input. The dual phase advance controllers provide superior performance in controlling the representative MSBS system when compared to the P I D controller. The choice of the feedback dual phase-advance controller as the "best" is based on the controller's suitability for a large gap MSBS system. The dual phase-advance controllers provide better stiffness than the P I D controllers.

The "best" of the forward path P I D controllers is the Mitsui Engineering and Shipbuilding, equation 4.8. This controller is derived using a quadratic fit. This type of quadratic fit transformation also produced the "best" overall feedback dual phase-advance controller from Loughborough, equation 4.7. These quadratic fit controllers are simple to derive when compared to some of the other controllers. A feature of the quadratic fit is the selection of strike time, $\zeta$, which influences the response of the system. This strike time can be chosen to optimize a given system's performance.

Nearly all the controllers have the same basic generic equation as shown below.

$$V_k = a_2\,\epsilon_{k+2} + a_1\,\epsilon_{k+1} + a_0\,\epsilon_k + a_{-1}\,\epsilon_{k-1} + a_{-2}\,\epsilon_{k-2} + b_{-1}\,V_{k-1} + b_{-2}V_{k-2}$$

The only difference is the method used to determine the coefficients and the coefficient values. The quadratic fit controllers provide both good control and a simple method of deriving the controller coefficients. The values of $\epsilon_{k+2}$ and $\epsilon_{k+1}$ are controller input values which are future values that have not occured. These values are predictive by the quadratic fit controllers.

## 7.2 Future Methods of Control

With the development of modern control theories, the application of state-space type controls to an MSBS is likely to be an extension for future controllers. As shown earlier, the linearized mathematical model of an MSBS is both observable and controllable. This allows the selection of any desired system performance by the pole placement methods. These pole locations are only limited to the ability of the power supply. Another advantage of a state-space controller is in the simplicity of implementing the controller algorithm on computers. As with digital simulation of analog controllers, the possibilities of state-space controllers are also unlimited.

One of the requirements for MSBS systems is the feedback signal to obtain stability. This feedback signal is usually body position, which is used to determine a velocity/derivative control signal. The idea of using acceleration feedback which can be integrated to obtain velocity and position is possible. The instrumentation to produce this feedback must be adaptable to strong magnetic fields. ONERA, in 1968, suspended a model with a telemetry package that included four accelerometers (Ref. 28). The response times of the controllers will improve using acceleration feedback. Work is presently underway to study the use of acceleration feedback in

an MSBS system. The final goal would be the development of an internal rate gyro to obtain all the position information of the model.

All the controllers discussed in this report are linear controllers which do provide adequate control of an MSBS system. An improvement in system performance can be obtained by the development of nonlinear or adaptive controllers. These controllers will be more complex to develop and program. Presently, some digital controllers do have nonlinear controls which limit the output command to the power supply so as not to exceed its capabilities. The need for nonlinear controllers is evident in the wind tunnel because of the large changes in forces or body orientation during a run. With the present controllers, a standard wind tunnel run requires the operator to change the controller gains when the forces on the body change. These gain changes are referred to as gain scheduling and have been used at the University of Southampton in obtaining high angle-of-attack suspension. (Ref. 16)

### 7.3 Effects that any Approximations may have on Results

Several approximations are made in the derivation of the governing equation for an MSBS system. These approximations are considered reasonable simplifications to the nonlinear equations of a true MSBS. Several reports have shown that the linear approximation gives a good representation of the MSBS dynamics (Ref. 4). These approximations apply well to the magnetic bearing systems and to the wind tunnel systems while operating at their equilibrium points. The equations do not adequately represent the dynamics during large position changes away from the equilibrium point. In practice, the controllers which are designed using the linear MSBS plant also adequately control the system during large position changes from equilibrium.

For any MSBS, the choice of a controller is extremely important because the controller will directly determine the performance of the system. However, the most important choice for any MSBS system is the available power supply. An ideal controller can have output commands that are beyond the capabilities of the power supply. It is possible to operate a system where

the power supply capabilities are low. Great care is required in the type of commands or loads applied to such a system. The limitations of the power supply are not usually a problem with magnetic bearings because of the low currents used. For the large gap MSBS, as in a wind tunnel, the power supply limitations are a continuing concern. The limitations of the power supply used to provide the required currents to the suspension coils have not been covered extensively. This could allow a controller to be chosen as the "best" which requires more power than is available. A designer should be constantly aware in the choice of the best controller.

## 7.4 Applications to Multi-Degree of Freedom System

In a multi-degree-of-freedom system, several controllers must act together to maintain stability. For a multi-degree-of-freedom system, the relation of the magnetic forces to body position are highly coupled and largely dependent on the arrangement of the coils. Decoupling of this relation into the required degrees-of-freedom is required for control. This decoupling is presently done for all MSBS associated with wind tunnels with good results in controlling a specific degree-of-freedom. There is a slight coupling between some degrees-of-freedom; however, this quickly dies out in a few computational cycles.

## REFERENCES


1. Holmes, F. T.: Axial Magnetic Suspension. Review of Scientific Instruments, Vol. 8, November 1937.

2. Tournier, Marcel; and Laurenceau, P.: Suspension Magnetique d'une Maquette en Soufflerie. (Magnetic Suspension of a Model in a Wind Tunnel.) La Recherche Aeronautique, No. 59, July - August 1957.

3. Boyden, R. P.: A Review of Magnetic Suspension and Balance Systems. AIAA 15th Aerodynamic Testing Conference, San Diego, California, May 18-20, 1988.

4. Tuttle, Marie H.; Kilgore, Robert A.; and Boyden, Richmond P.: Magnetic Suspension and Balance Systems. A Selected, Annotated Bibliography. NASA Technical Memorandum 84661, February 1988.

5. Vyshkov, I. D.; Koval'nogov, S. A.; Usachev, V. N.; and Shapovalov, G. K.: A System for the Electromagnetic Levitation of Models in a Subsonic Wind Tunnel. TsAGI, Uchenye Zapiski (ISSn\N 0321-3429), Vol. 17, No. 4, 1986, pp. 94-97. In Russian.

6. Humphris, R. R.; Kelm, R. D.; Lewis, D. W.; and Allaire, P. E.: Effects of Control Algorithms on Magnetic Journal Bearing Properties. ASME Vol. 108, October 1986, pp. 624-632

7. Sinha, P. K.: Electromagnetic Suspension; Dynamics and Controls. Peter Peregrinus Ltd., United Kingdom, 1987.

8. Lowther, D. A.; and Silvester, P. P.: Computer-Aided Design in Magnetics. Springer-Verlag, New York, 1986.

9. Britcher, C. P.; Goodyer, M. J.; Eskins, J.; Parker, D.; and Halford, R. J.: Digital Control of Wind Tunnel Magnetic Suspension and Balance Systems. Proceedings of the ICIASF Record - International Congress on Instrumentation in Aerospace Simulation Facilities, Williamsburg, Virginia, June 22-25, 1987.

10. D'Azzo, John J.; and Houpis, Constantine H.: Feedback Control System Analysis and Synthesis, 2nd Edition. McGraw-Hill Book Company, New York, 1966.

11. Altmann, H.: An Optical Scanning Detection System and its Use with a Magnetic Suspension System for Low Density Sphere Drag Measurements. In the 2nd International Symposium on Electro-Magnetic Suspension, Southampton, England, July 12-14, 1971.

12. Haslam-Jones, T. F.: Measurement of the Drag of Slender Cones in Hypersonic Flow at Low Reynolds Number Using a Magnetic Suspension and Balance. University of Oxford, Department of Engineering, Science Report 1235/78, March 1979.

13. Luh, Peter B.; Covert, Eugene E.; Whitaker, H. Phillips; and Haldeman, Charles W.: Application of Digital Control to a Magnetic Model Suspension and Balance System. Final Report, April 1, 1976 - November 30, 1977. MIT-TR-198, December 1977, NASA CR 145316, January 1978.

14. Fortescue, P. W.; and Bouchalis, C.: Digital Controllers for the Vertical Channels of a Magnetic Suspension System, NASA CR 165684, May 1981.

15. Britcher, C. P.: The Southampton University Magnetic Suspension and Balance System - A Partial User Guide. Southampton University Department of Aeronautics and Astronautics AASU Tech., Memo 83/8, April 1984.

16. Parker, D.;and Britcher, C. P.: Progress Toward Extreme Attitude Testing with Magnetic Suspension and Balance Systems. AIAA 15th Aerodynamic Testing Conference, San Diego, California, May 18-20, 1988.

17. Britcher, C. P.: User Guide for the Digital Control System of the NASA/Langley Research Center's 13-Inch Magnetic Suspension and Balance System. Old Dominion University Research Foundation, NASA CR 178210, March 1987.

18. Sawada, Hideo; Kanda, Hiroshi; and Suenaga, Hisashi: A Position and Attitude Sensing Camera in NAL's MSBS. MSBS Newsletter published by the Experimental Techniques Branch, NASA Langley Research Center, No. 4, January 1988.

19. Carmichael, A. T.; Hinchliffe, S.; Murgatroyd, P. N.; and Williams, I. D.: Magnetic Suspension Systems with Digital Controllers. Review of Scientific Instruments, Vol. 57, No. 8, August 1986.

20. Matsuda, R.; Nakagawa, M.; and Yamada, I.: Multi Input-Output Control of a Magnetically Suspended Linear Guide. IEEE Transactions on Magnetics, MAG-20, No. 5, September 1984.

21. Hisatani, M.; Inoue, Y.;and Mitsui, J.: Development of Digitally Controlled Magnetic Bearing. Bulletin of Japan Society of Mechanical Engineering, Vol. 29, No. 247, January 1986.

22. Hornbeck, Robert W.: Numerical Methods. Prentice-Hall, Inc., New Jersey, USA, 1975.

23. Scudiere, M. B.; Willems, R. A.; and Gillies, G. T.: Digital Controller for a Magnetic Suspension System. Review of Scientific Instruments, Vol. 57, No. 8, August 1986.

24. Keith, F. J.; Williams, R. D.; Allaire, P. E.; and Schafer, R.M.: Digital Control of Magnetic Bearings Supporting a Multimass Flexible Rotor. University of Virginia, Electrical Engineering Department, Virginia, 1988.

25. Lawson, M. A.; and Gillies, G. T.: Interrupt-Driven Digital Controllers for a Magnetic Suspension System. Review of Scientific Instruments, Vol. 60, No. 3, March 1989.

26. Franklin, G.F.; Powell, J.D.; and Emami-Naeini, Abbas: Feedback Control of Dynamic Systems. Addison-Wesley Publishing Company Inc., Massachusetts, 1986.

27. Microsoft QuickBASIC Version 4.5. Microsoft Corporation 1988.

28. Beaussler, J.;and Zakneim, J.: Telemetrie Multivoies pour Maquettes en Suspension Magnetique. (Multichannel Telemetering Device for Magnetically Suspended Models) Presented at the Colloquium on the Properties and the Behavior of Electronic Components and Assemblies Submitted to Strong Accelerations. Saint-Louis, France. October 1968.

## APPENDIX A

Program Listing

The simulation program is written in Microsoft Quick Basic, Version 4.5. Below is a block diagram of the controller and MSBS plant used in this program.

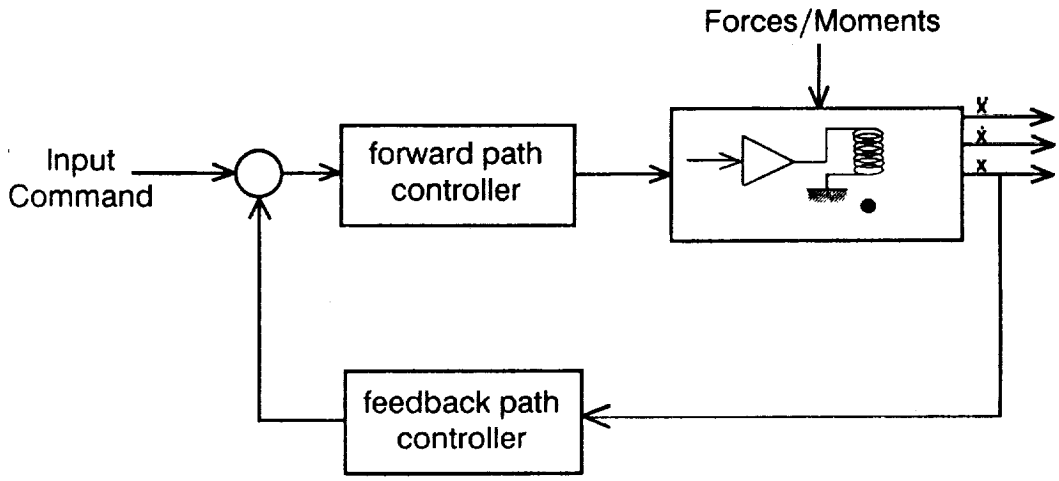

This program displayed and saved the position trajectories of a simulation run. Below is a printout of the program's display.

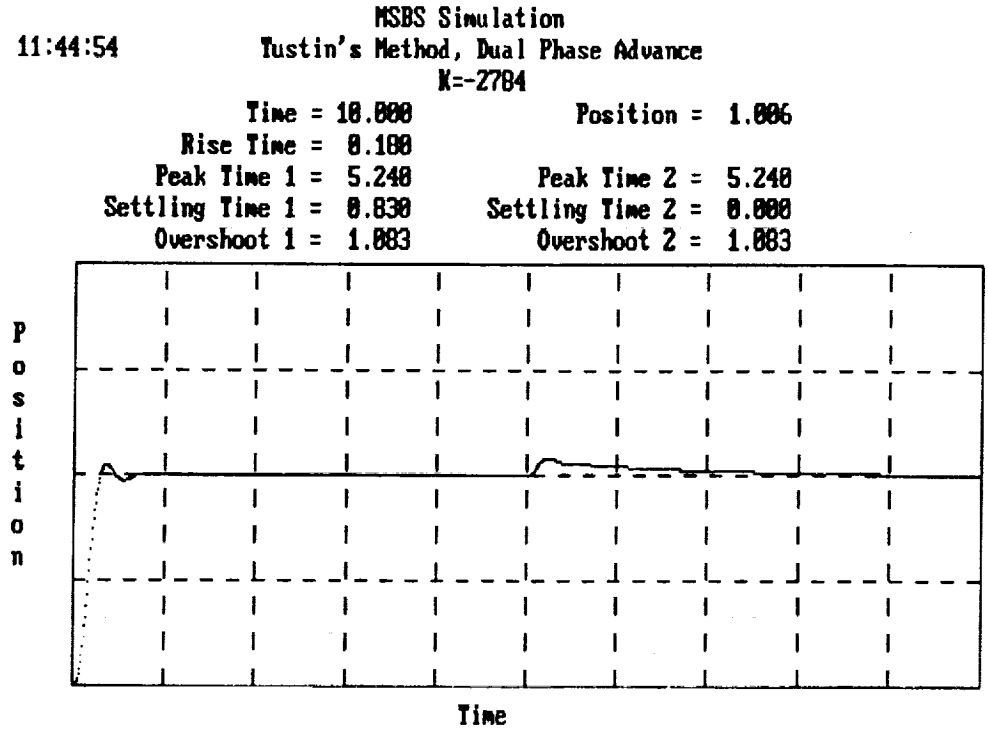


(Program Listing)

```
CLS
CLEAR
'Saved as MSBSSIM.BAS
'OPEN "B:filename" FOR OUTPUT AS #1
'Sampling Time
T = .01
'The MSBS plant variables
Kx = -1
Kc = -.1
Ki = .1
m = 1
R = 1
L = .1
C = 0
'The MSBS plant coefficients
a0 = -Ki / m / L
a1 = R / m / L + 2 / m / T
a2 = 3 * R / m / L + 2 / m / T
a3 = 3 * R / m / L - 2 / m / T
a4 = R / m / L - 2 / m / T
b0 = (2/T)^3+(2/T)^2*(R/L+C/m)+2/T*(C*R/m/L+Kx/m-Ki*Kc/L/m)+R*Kx/L/m
b1 = -3*(2/T)^3-(2/T)^2*(R/L+C/m)+2/T*(C*R/m/L+Kx/m-Ki*Kc/L/m)+3*R*Kx/L/m
b2 = 3*(2/T)^3-(2/T)^2*(R/L+C/m)-2/T*(C*R/m/L+ Kx/m- Ki*Kc/L/m)+3*R*Kx/L/m
```

```
b3 = -(2/T)^3+(2/T)^2*(R/L+C/m)-2/T*(C*R/m/L+Kx/m-Ki*Kc/L/m)+R*Kx/L/m
'Screen layout
tmax = 20
tmin = 0
XMAX = 2
xmin = 0
SCREEN 9
COLOR 14, 1
VIEW (40, 125)-(620, 320), 9
WINDOW (tmin-.01*tmax, xmin-.02*XMAX)-(tmax+.01*tmax, XMAX+.02*XMAX)
'Borders
 LINE (tmin, xmin)-(tmin, XMAX), 14
 LINE (tmin, xmin)-(tmax, xmin), 14
 LINE (tmin, XMAX)-(tmax, XMAX), 14
 LINE (tmax, xmix)-(tmax, XMAX), 14
'Horizontal lines
 LINE (tmin, .25 * XMAX)-(tmax, .25 * XMAX), 8, , &HFF00
 LINE (tmin, .5 * XMAX)-(tmax, .5 * XMAX), 11, , &HFF00
 LINE (tmin, .75 * XMAX)-(tmax, .75 * XMAX), 8, , &HFF00
'Vertical lines
 LINE (tmax * .1, xmin)-(tmax * .1, XMAX), 8, , &HFF00
 LINE (tmax * .2, xmin)-(tmax * .2, XMAX), 8, , &HFF00
 LINE (tmax * .3, xmin)-(tmax * .3, XMAX), 8, , &HFF00
 LINE (tmax * .4, xmin)-(tmax * .4, XMAX), 8, , &HFF00
 LINE (tmax * .5, xmin)-(tmax * .5, XMAX), 8, , &HFF00
 LINE (tmax * .6, xmin)-(tmax * .6, XMAX), 8, , &HFF00
 LINE (tmax * .7, xmin)-(tmax * .7, XMAX), 8, , &HFF00
 LINE (tmax * .8, xmin)-(tmax * .8, XMAX), 8, , &HFF00
 LINE (tmax * .9, xmin)-(tmax * .9, XMAX), 8, , &HFF00
'Label
LOCATE 12, 2: PRINT "P"
LOCATE 13, 2: PRINT "o"
LOCATE 14, 2: PRINT "s"
LOCATE 15, 2: PRINT "i"
LOCATE 16, 2: PRINT "t"
LOCATE 17, 2: PRINT "i"
LOCATE 18, 2: PRINT "o"
LOCATE 19, 2: PRINT "n"
LOCATE 2, 30: PRINT "MSBS Simulation"
'Input step of position
ref = 1
LOCATE 3, 2: PRINT TIME$
52 Total = Total + T
'GOSUB 100   'Tustin's D P A, equation (B-3) feedback path
'GOSUB 250   'NASA D P A, equations (4.4a), (4.4b), and (4.4c) feedback path
'GOSUB 300   'Southampton D P A, equations (4.2c), and (4.2d) feedback path
'GOSUB 450   'Loughborough D P A, equation (4.7) feedback path
'GOSUB 475   'Loughborough D P A, equation (4.7) feedback path
'GOSUB 525   'UVa P D, equation (4.16) feedback path
'GOSUB 550   'UVa P D, equation (4.16) forward path
'GOSUB 600   'Japan P I D, equation (4.8) forward path
```

```
    'GOSUB 650   'Japan P D, and I, equation (4.8) feedback path
    'GOSUB 750   'Japan P I D, equation (4.11) forward path
    'GOSUB 800   'Japan P I D, equation (4.10) forward path
    GOSUB 850   'UVa P I D, equation (4.17) forward path
    'GOSUB 900   'Oak Ridge P I D, equation (4.13) forward path, (Not Working)
    'GOSUB 1000  'Oak Ridge P I D, equation (4.15) forward path, (Not Working)
    'GOSUB 1100  'Tustin's P I D, equation (B-5) forward path
    'Total Error Sum
    SUError = ABS(Xp1 - X) / ref + SUError
    'Max. Overshoot and Peak Time for Position Input
     IF X > MAXX THEN MAXX = X
     IF X = MAXX THEN PTIME = Total
    'Max. Overshoot and Peak Time for Force Input
    IF Total > 5 AND X > MAX2 THEN MAX2 = X
    IF X = MAX2 THEN PTIME2 = Total
    'Rise Time
    IF X <= (.1 * ref) THEN RT1 = Total
    IF jj = 1 THEN GOTO 98
    IF X >= (.9 * ref) THEN jj = 1
    IF X >= (.9 * ref) AND jj = 1 THEN RT2 = Total
    RISE = RT2 - RT1
    LOCATE 6,15: PRINT "Rise Time =": LOCATE 6,27: PRINT USING "##.###"; RISE
98  LOCATE 9,13: PRINT "Overshoot 1 =": LOCATE 9,27: PRINT USING "##.###"; MAXX
    LOCATE 7,13: PRINT "Peak Time 1 =": LOCATE 7,27: PRINT USING "##.###"; PTIME
    LOCATE 7,43: PRINT "Peak Time 2 =": LOCATE 7,57: PRINT USING "##.##"; PTIME2
    LOCATE 5,20: PRINT "Time =": LOCATE 5,26: PRINT USING " ##.###"; Total
    LOCATE 5,46: PRINT "Position =": LOCATE 5,57: PRINT USING "##.###"; X
    LOCATE 9,43: PRINT "Overshoot 2 =": LOCATE 9,57: PRINT USING "##.###"; MAX2
    'Position Input Settling Time
    p = .001
    IF jjj = 1 THEN GOTO 59
    IF (ABS(Xp1-X)<p*X) AND (ABS(Xp2-X)<p*X) AND (ABS(Xp3-X)<p*X) AND (ABS(Xp4-
    X)<p*X) AND (ABS(Xp5-X)<p*X) AND (ABS(XP6-X)<p*X) AND (ABS(Xp7-X)<p*X) AND
    (ABS(Xp8-X)<p*X) THEN SETTIME = Total
    IF SETTIME = Total THEN jjj = 1
    LOCATE 8,9: PRINT"SettlingTime 1 = ":
    LOCATE 8,27: PRINT USING " ##.### ";SETTIME
59  'Force Input Settling Time
    pp = .0005
    IF jjjj = 1 THEN GOTO 70
    IF fd > 1 THEN GOTO 60 ELSE GOTO 70
60  IF ABS(X - ref) / ref < pp AND ABS(Xp1 - ref) / ref < pp AND ABS(Xp2 - ref) / ref < pp
    AND ABS(Xp3 - ref) / ref < pp AND ABS(Xp4 - ref) / ref < pp AND ABS(Xp5 - ref) / ref <
    pp AND ABS(XP6 - ref) / ref < pp AND ABS(Xp7 - ref) / ref < pp AND ABS(Xp8 - ref) / ref
    < pp THEN SETTIME2 = Total
    IF SETTIME2 = Total AND Total > 6 THEN jjjj = 1
    LOCATE 8,39: PRINT "Settling Time 2 =":
    LOCATE 8,57: PRINT USING "##.### "; SETTIME2
    'Shift the variables back in time
70  fdp3 = fdp2
    fdp2 = fdp1
```

```
    fdp1 = fd
    Xp8 = Xp7
    Xp7 = XP6
    XP6 = Xp5
    Xp5 = Xp4
    Xp4 = Xp3
    Xp3 = Xp2
    Xp2 = Xp1
    Xp1 = X
    Ep3 = Ep2
    Ep2 = Ep1
    Ep1 = E
    Vp3 = Vp2
    Vp2 = Vp1
    Vp1 = V
    PSET (Total, X), 15:
    'PRINT #1, USING " ###.###"; Total; X
    'Input step of force
    IF Total > 5 THEN fd = 10
    IF Total > tmax AND Total < tmax + T THEN GOTO 80 ELSE GOTO 52
80  LOCATE 24, 37: PRINT "Time"
    BEEP
    LOCATE 3, 2: PRINT TIME$
    CLOSE
88  END

    'Subroutines
100 'Tustin's D P A, equation (B-3), feedback path, plus error integrator
    IF first = 1 GOTO 110
    K = -2784
    LOCATE 3, 21: PRINT "Tustin's D P A, equation (B-3)"
    LOCATE 4, 35: PRINT "K="; K
    BEEP
    gain = 1
    Kin = .5
    A = .01
    n = 10
    c0 = (T * T + 4 * n * A * T + 4 * n * n * A * A) / (T * T + 4 * A * T + 4 * A * A)
    c1 = (2 * T * T - 8 * n * n * A * A) / (T * T + 4 * A * T + 4 * A * A)
    c2 = (T * T - 4 * n * A * T + 4 * n * n * A * A) / (T * T + 4 * A * T + 4 * A * A)
    c3 = (2 * T * T - 8 * A * A) / (T * T + 4 * A * T + 4 * A * A)
    c4 = (T * T - 4 * A * T + 4 * A * A) / (T * T + 4 * A * T + 4 * A * A)
    d1 = Kin * T
110 E = ref * gain - G
    Etotal = E + Etotal
    Z = E + d1 * Etotal
    V = K * Z
    X = (a0*(V+Vp1+Vp2+Vp3)+a1*fd+a2*fdp1+a3*fdp2+a4*fdp3-b1*Xp1-b2*Xp2-b3*Xp3)/b0
    G = c0 * X + c1 * Xp1 + c2 * Xp2 - c3 * Gp1 - c4 * Gp2
    Gp2 = Gp1
    Gp1 = G
```

```
    first = 1
    RETURN

250 'NASA D P A, equations (4.4a), (4.4b), and (4.4c), feedback path, plus error integrator
    IF first = 1 GOTO 260
    K = -2777
    LOCATE 3, 26: PRINT "NASA D P A, equations (4.4a), (4.4b), and (4.4c)"
    LOCATE 4, 35: PRINT "K="; K
    BEEP
    gain = 1
    Kin = .8
    A = .01
    n = 10
    c1 = A / (T + A)
    c2 = (T * T) / (A * A)
    c3 = 1 + n * A / T
    c4 = -n * A / T
    d1 = Kin * T
    d2 = c1 * c3 * c2
    d3 = c1 * c4 * c2
    d4 = c1 * c3
    d5 = c1 * c4
260 E = ref * gain - G
    Etotal = E + Etotal
    Z = E + d1 * Etotal
    V = K * Z
    X=(a0*(V+Vp1+Vp2+Vp3)+a1*fd+a2*fdp1+a3*fdp2+a4*fdp3-b1*Xp1-b2*Xp2- b3*Xp3)/b0
    UU = d2 * X + d3 * Xp1 + c1 * UUp1
    G = d4 * UU + d5 * UUp1 + c1 * Gp1
    UUp1 = UU
    Gp1 = G
    first = 1
    RETURN

300 'Southampton D P A, equations (4.2c) and (4.2d), feedback path, plus error integrator
    IF first = 1 GOTO 310
    K = -2665
    LOCATE 3, 22: PRINT "Southampton D P A, equation (4.2c), and (4.2d)"
    LOCATE 4, 35: PRINT "K="; K
    BEEP
    gain = 1
    Kin = .5
    A = .01
    n = 10
    c1 = T / (A + T)
    c2 = A / (A + T)
    c3 = (T + n * A) / T
    c4 = -n * A / T
    d1 = Kin * T
    d2 = c3 * c1
    d3 = c4 * c1
```

```
310 E = ref * gain - G
    Etotal = E + Etotal
    Z = E + d1 * Etotal
    V = K * Z
    X=(a0*(V+Vp1+Vp2+Vp3)+a1*fd+a2*fdp1+a3*fdp2+a4*fdp3-b1*Xp1-b2*Xp2-b3*Xp3)/b0
    UU = c2 * UUp1 + d2 * X + d3 * Xp1
    G = c2 * Gp1 + d2 * UU + d3 * UUp1
    UUp1 = UU
    Gp1 = G
    first = 1
    RETURN

450 'Loughborough D P A, equation (4.7), feedback path, plus error integrator
    IF first = 1 GOTO 460
    K = -2080
    LOCATE 3, 19: PRINT "Loughborough D P A, equation (4.7)"
    LOCATE 4, 35: PRINT "K="; K
    BEEP
    gain = 1
    Kin = .5
    zeta = 1.5
    A = .01
    n = 10
    aL0=(1+3*zeta/2+3*n*A/T+zeta^2/2+2*n*A*zeta/T+n*n*A*A/T/T)/(1+3*A/T+A*A/T/T)
    aL1=(-2*zeta-4*n*A/T-zeta^2-4*n*A*zeta/T-2*n*n*A*A/T/T)/(1+3*A/T+A*A/T/T)
    aL2=(zeta/2+n*A/T+zeta^2/2+2*n*A*zeta/T+n*n*A*A/T/T)/(1+3*A/T+A*A/T/T)
    bL0 = (4 * A / T + 2 * A * A / T / T) / (1 + 3 * A / T + A * A / T / T)
    bL1 = -1 * (A / T + A * A / T / T) / (1 + 3 * A / T + A * A / T / T)
    d1 = Kin * T
460 E = ref * gain - G
    Etotal = E + Etotal
    Z = E + d1 * Etotal
    V = K * Z
    X=(a0*(V+Vp1+Vp2+Vp3)+a1*fd+a2*fdp1+a3*fdp2+a4*fdp3-b1*Xp1-b2*Xp2-b3*Xp3)/b0
    G = aL0 * X + aL1 * Xp1 + aL2 * Xp2 + bL0 * Gp + bL1 * Gp1
    Gp1 = Gp
    Gp = G
    first = 1
    RETURN

475 'Loughborough D P A, equation (4.7), forward path, plus error integrator
    IF first = 1 GOTO 460
    K = -3115
    LOCATE 3, 19: PRINT "Loughborough D P A, equation (4.7)"
    LOCATE 4, 35: PRINT "K="; K
    BEEP
    gain = 1
    Kin = .5
    zeta = 1.5
    A = .01
    n = 10
```

```
    aL0=(1+3*zeta/2+3*n*A/T+zeta^2/2+2*n*A*zeta/T+n*n*A*A/T/T)/(1+3*A/T+A*A/T/T)
    aL1=(-2*zeta-4*n*A/T-zeta^2-4*n*A*zeta/T-2*n*n*A*A/T/T)/(1+3*A/T+A*A/T/T)
    aL2=(zeta/2+n*A/T+zeta^2/2+2*n*A*zeta/T+n*n*A*A/T/T)/(1+3*A/T+A*A/T/T)
    bL0 = (4 * A / T + 2 * A * A / T / T) / (1 + 3 * A / T + A * A / T / T)
    bL1 = -1 * (A / T + A * A / T / T) / (1 + 3 * A / T + A * A / T / T)
    d1 = Kin * T
495 E = ref * gain - G
    Etotal = E + Etotal
    ZZ = aL0 * E + aL1 + aL2 * Ep2 + bL0 * ZZp + bL1 * ZZp1
    Z = ZZ + d1 * Etotal
    V = K * Z
    X=(a0*(V+Vp1+Vp2+Vp3)+a1*fd+a2*fdp1+a3*fdp2+a4*fdp3-b1*Xp1-b2*Xp2-b3*Xp3)/b0
    ZZp1 = ZZp
    ZZp = ZZ
    G = X
    first = 1
    RETURN

525 'UVa P D, equation (4.16), feedback path, plus error integrator
    IF first = 1 GOTO 535
    K = -405
    LOCATE 4, 35: PRINT "K="; K
    LOCATE 3, 20: PRINT "UVa P D, equation (4.16)"
    BEEP
    gain = 1
    Kp = 1
    Kd = .4
    Kin = .5
    c1 = Kd / T
    c2 = Kp + c1
    d1 = Kin * T
535 E = ref * gain - G
    Etotal = E + Etotal
    Z = E + d1 * Etotal
    V = K * Z
    X=(a0*(V+Vp1+Vp2+Vp3)+a1*fd+a2*fdp1+a3*fdp2+a4*fdp3-b1*Xp1-b2*Xp2-b3*Xp3)/b0
    G = c2 * X - c1 * Xp1
    first = 1
    RETURN

550 'UVa P D, equation (4.16), forward path, plus error integrator
    IF first = 1 GOTO 560
    K = -361
    LOCATE 3, 22: PRINT "UVa P D, equation (4.16)"
    LOCATE 4, 35: PRINT "K="; K
    BEEP
    gain = 1
    Kp = 1
    Kd = .4
    Kin = .5
    c1 = Kd / T
```

```
    c2 = Kp + c1
    d1 = Kin * T
560 E = ref * gain - G
    Etotal = E + Etotal
    ZZ = d1 * Etotal
    Z = c2 * E - c1 * Ep1 + ZZ
    V = K * Z
    X=(a0*(V+Vp1+Vp2+Vp3)+a1*fd+a2*fdp1+a3*fdp2+a4*fdp3-b1*Xp1-b2*Xp2-b3*Xp3)/b0
    G = X
    first = 1
    RETURN

600 'Japan P I D, equation (4.8), forward path
    IF first = 1 GOTO 610
    K = -522
    LOCATE 3, 15: PRINT "Japan P I D, equation (4.8)"
    LOCATE 4, 35: PRINT "K="; K
    BEEP
    gain = 1
    Kp = 1
    Kd = .4
    Kin = .5
    c1 = 15 * Kp / 8 + 2 * Kd / T
    c2 = 42 * Kp / 8 + 5 * Kd / T
    c3 = 35 * Kp / 8 + 3 * Kd / T
    d1 = Kin * T
610 E = ref * gain - G
    Etotal = E + Etotal
    Z = c1 * Ep2 - c2 * Ep1 + c3 * E + d1 * Etotal
    V = K * Z
    X=(a0*(V+Vp1+Vp2+Vp3)+a1*fd+a2*fdp1+a3*fdp2+a4*fdp3-b1*Xp1-b2*Xp2-b3*Xp3)/b0
    G = X
    first = 1
    RETURN

650 'Japan P D and I, equation (4.8), feedback path, plus error integrator
    IF first = 1 GOTO 660
    K = -391
    LOCATE 3, 15: PRINT "Japan, P D, and I, equation (4.8)"
    LOCATE 4, 35: PRINT "K="; K
    BEEP
    gain = 1
    Kp = 1
    Kd = .4
    Kin = .5
    c1 = 15 * Kp / 8 + 2 * Kd / T
    c2 = 42 * Kp / 8 + 5 * Kd / T
    c3 = 35 * Kp / 8 + 3 * Kd / T
    d1 = Kin * T
660 E = ref * gain - G
    Etotal = E + Etotal
```

```
    Z = E + d1 * Etotal
    V = K * Z
    X=(a0*(V+Vp1+Vp2+Vp3)+a1*fd+a2*fdp1+a3*fdp2+a4*fdp3-b1*Xp1-b2*Xp2-b3*Xp3)/b0
    Xtotal = X + Xtotal
    G = c1 * Xp2 - c2 * Xp1 + c3 * X
    first = 1
    RETURN

750 'Japan P I D, equation (4.11), forward path
    IF first = 1 GOTO 760
    K = -360
    LOCATE 3, 18: PRINT "Japan P I D, equation (4.11)"
    LOCATE 4, 35: PRINT "K="; K
    BEEP
    gain = 1
    Kp = 1
    Kd = .4
    Kin = .5
    aJ2 = -Kp / 12 - Kd / (12 * T)
    aJ1 = 8 * Kp / 12 + 16 * Kd / (12 * T)
    aJ0 = Kin * T - 30 * Kd / (12 * T)
    aJp1 = -8 * Kp / 12 + 16 * Kd / (12 * T)
    aJp2 = Kp / 12 - Kd / (12 * T)
    c1 = 5 * aJ2 + 2 * aJ1 - aJp1 - aJp2
    c2 = 3 * aJ2 + aJ1 + aJp2
    c3 = aJ2 + aJ1 + aJ0 + aJp1 + aJp2
760 E = ref * gain - G
    Etotal = E + Etotal
    Z = c1 * E - c2 * Ep1 + c3 * Etotal
    V = K * Z
    X=(a0*(V+Vp1+Vp2+Vp3)+a1*fd+a2*fdp1+a3*fdp2+a4*fdp3-b1*Xp1-b2*Xp2-b3*Xp3)/b0
    G = X
    first = 1
    RETURN

800 'Japan P I D, equation (4.10), forward path
    IF first = 1 GOTO 810
    K = -359
    LOCATE 3, 15: PRINT "Japan P I D, equation (4.10)"
    LOCATE 4, 35: PRINT "K="; K
    BEEP
    gain = 1
    Kp = 1
    Kd = .4
    Kin = .5
    aJ2 = -Kp / 12 - Kd / (12 * T)
    aJ1 = 8 * Kp / 12 + 16 * Kd / (12 * T)
    aJ0 = Kin * T - 30 * Kd / (12 * T)
    aJp1 = -8 * Kp / 12 + 16 * Kd / (12 * T)
    aJp2 = Kp / 12 - Kd / (12 * T)
    c1 = 6 * aJ2 + 3 * aJ1 + aJ0
```

```
    c2 = -8 * aJ2 - 3 * aJ1 + aJp1
    c3 = 3 * aJ2 + aJ1 + aJp2
810 E = ref * gain - G
    Z = c1 * E + c2 * Ep1 + c3 * Ep2 + Zp1
    V = K * Z
    X=(a0*(V+Vp1+Vp2+Vp3)+a1*fd+a2*fdp1+a3*fdp2+a4*fdp3-b1*Xp1-b2*Xp2-b3*Xp3)/b0
    Zp1 = Z
    G = X
    first = 1
    RETURN

850 'UVa P I D, equation (4.17), forward path
    IF first = 1 GOTO 860
    K = -359
    LOCATE 3, 22: PRINT "UVa P I D, equation (4.17)"
    LOCATE 4, 35: PRINT "K="; K
    BEEP
    gain = 1
    Kp = 1
    Kd = .4
    Kin = .5
    c1 = Kp + Kd / T
    c2 = -Kd / T
    d1 = T / 2
860 E = ref * gain - G
    Etotal = Etotal + d1 * (E + Ep1)
    Z = c1 * E + c2 * Ep1 + Kin * Etotal
    V = K * Z
    X=(a0*(V+Vp1+Vp2+Vp3)+a1*fd+a2*fdp1+a3*fdp2+a4*fdp3-b1*Xp1-b2*Xp2-b3*Xp3)/b0
    G = X
    RETURN

900 'Oak Ridge P I D, equation (4.13), forward path
    IF first = 1 GOTO 910
    K = -100
    LOCATE 3, 19: PRINT "Oak Ridge P I D, equation (4.13)"
    LOCATE 4, 35: PRINT "K="; K
    BEEP
    gain = 1
    Kp = 1
    Kd1 = .4
    Kd2 = .4
    Kin = .5 * T
    W = .5
    dd0 = 1 - W ^ 3
    dd1 = 3 / 2 * (1 - W) ^ 2 * (1 + W)
    dd2 = 1 / 2 * (1 - W) ^ 2
910 E = ref * gain - G
    dE = E - da0
    Etotal = E + Etotal
    da0 = da0 + dd0 * dE
```

```
     da1 = da1 + dd1 * dE
     da2 = da2 + dd2 *dE
     Z = Kp * E + Kd1 * da1 + 2 * Kd2 * da2+ Kin * Etotal
     V = K * Z
     X=(a0*(V+Vp1+Vp2+Vp3)+a1*fd+a2*fdp1+a3*fdp2+a4*fdp3-b1*Xp1-b2*Xp2-b3*Xp3)/b0
     G = X
     first = 1
     RETURN

1000 'Oak Ridge P I D, equation (4.15), forward path
     IF first = 1 GOTO 1010
     K = -400
     LOCATE 3, 19: PRINT "Oak Ridge P I D, equation (4.15)"
     LOCATE 4, 35: PRINT "K="; K
     BEEP
     gain = 1
     Kp = 1
     Kpp = 1
     Kd1 = .4
     Kd2 = .4
     Kdp1 = .4
     Kdp2 = .4
     Kin = .5 * T
     W = .5
     dd0 = 1 - W ^ 3
     dd1 = 3 / 2 * (1 - W) ^ 2 * (1 + W)
     dd2 = 1 / 2 * (1 - W) ^ 2
1010 E = ref * gain - G
     dE = E - da0
     Etotal = E + Etotal
     da0 = da0 + dd0 * dE
     da1 = da1 + dd1 * dE
     da2 = da2 + dd2 * dE
     da0p = da0 + da1 + da2
     da1p = da1 + 2 * da2
     da2p = da2
     Z = Kpp*da0p+Kp*da0+Kdp1*da1p+2*Kdp2*da2p+Kd1*da1+2*kd2*da2+Kin*Etotal
     V = K * Z
     X=(a0*(V+Vp1+Vp2+Vp3)+a1*fd+a2*fdp1+a3*fdp2+a4*fdp3-b1*Xp1-b2*Xp2-b3*Xp3)/b0
     G = X
     first = 1
     RETURN

1100 'Tustin's P I D, equation (B-5), forward path
     IF first = 1 GOTO 1110
     K = -396
     LOCATE 3, 22: PRINT "Tustin's P I D, equation (B-5)"
     LOCATE 4, 35: PRINT "K="; K
     BEEP
     gain = 1
     Kp = 1
```

```
      Kd = .4
      Kin = .5
      c1 = Kp + 2 * Kd / T + T * Kin / 2
      c2 = T * Kin - 4 * Kd / T
      c3 = T * Kin / 2 + 2 * Kd / T - Kp
1110  E = ref * gain - G
      Z = c1 * E + c2 * Ep1 + c3 * Ep2 + Zp2
      V = K * Z
      X=(a0*(V+Vp1+Vp2+Vp3)+a1*fd+a2*fdp1+a3*fdp2+a4*fdp3-b1*Xp1-b2*Xp2-b3*Xp3)/b0
      G = X
      Zp2 = Zp1
      Zp1 = Z
      first = 1
      RETURN
```

## APPENDIX B

Tustin's Method of Transformation

The Tustin's transformation is a transformation from the *S*-domain to the *z*-domain by substituting into the *S*-domain equation:

$$S = \frac{2}{T}\frac{(z-1)}{(z+1)}, \text{ where T is the sampling time} \tag{B-1}$$

The Tustin's transformation is only an approximation between the *S*-domain and *z*-domain which is based on the trapezoidal integration formula. This transformation gives good results as long as the sampling rate is high.

For a dual phase-advance controller given as:

$$\frac{V}{\epsilon} = \left(\frac{1 + nA\,S}{1 + A\,S}\right)^2 = \frac{1 + 2nA\,S + (nA\,S)^2}{1 + 2A\,S + (A\,S)^2} \tag{B-2}$$

then substituting in the Tustin's transformation of equation B-1, the dual phase-advance has the form:

$$V_k = a_0\epsilon_k + a_1\epsilon_{k-1} + a_2\epsilon_{k-2} - b_1V_{k-1} - b_2V_{k-2} \tag{B-3}$$

where:

$$a_0 = \frac{(T^2 + 4nAT + 4nA^2)}{(T^2 + 4AT + 4A^2)} \qquad b_1 = \frac{(2T^2 - 8A^2)}{(T^2 + 4AT + 4A^2)}$$

$$a_1 = \frac{(2T^2 - 8nA^2)}{(T^2 + 4AT + 4A^2)} \qquad b_2 = \frac{(T^2 - 4AT + 4A^2)}{(T^2 + 4AT + 4A^2)}$$

$$a_2 = \frac{(T^2 - 4nAT + 4nA^2)}{(T^2 + 4AT + 4A^2)}$$

For a P I D controller given as:

$$\frac{V}{\epsilon} = K\left[K_p + K_d\, S + \frac{K_{in}}{S}\right] \tag{B-4}$$

then substituting in the Tustin's transformation of equation B-4, the P I D has the form:

$$V_k = a_0\epsilon_k + a_1\epsilon_{k-1} + a_2\epsilon_{k-2} + V_{k-2} \tag{B-5}$$

where:

$$a_0 = K_p + \frac{2\,K_d}{T} + \frac{K_{in}T}{2} \qquad a_1 = K_{in}T - \frac{4\,K_d}{T} \qquad a_2 = \frac{K_{in}T}{2} + \frac{2\,K_d}{T} - K_p$$

The equations B-3 and B-5 are used as the Tustin's controller algorithms in the simulation program.

The dual phase-advance controller described by equation B-3 is referred to as Tustin's D P A. The P I D controller described by equation B-5 is referred to as Tustin's P I D.

NASA
National Aeronautics and Space Administration

# Report Documentation Page

| 1. Report No. | 2. Government Accession No. | 3. Recipient's Catalog No. |
|---|---|---|
| NASA CR-182087 | | |

**4. Title and Subtitle**

Comparison of Digital Controllers Used in Magnetic Suspension and Balance Systems

**5. Report Date**

December 1990

**6. Performing Organization Code**

**7. Author(s)**

William A. Kilgore

**8. Performing Organization Report No.**

**9. Performing Organization Name and Address**

Old Dominion University Research Foundation
P. O. Box 6369
Norfolk, Virginia 23608-0369

**10. Work Unit No.**

505-66-91-02

**11. Contract or Grant No.**

NAG-1-1056

**12. Sponsoring Agency Name and Address**

National Aeronautics and Space Administration
Langley Research Center
Hampton, VA 23665-5225

**13. Type of Report and Period Covered**

Progress Report
11/1/89 - 4/30/90

**14. Sponsoring Agency Code**

**15. Supplementary Notes**

Technical Monitor: Nelson J. Groom, Spacecraft Controls Branch, Guidance and Control Division
Principal Investigator: Colin P. Britcher, Old Dominion University Research Foundation

**16. Abstract**

Dynamic systems that were once controlled by analog circuits are now controlled by digital computers. Presented is a comparison of the digital controllers presently used with magnetic suspension and balance systems. The overall responses of the systems are compared using a computer simulation of the magnetic suspension and balance system and the digital controllers. The comparisons include responses to both simulated force and position inputs. A preferred digital controller is determined from the simulated responses.

| 17. Key Words (Suggested by Author(s)) | 18. Distribution Statement |
|---|---|
| Magnetic Suspension<br>Digital Control | Unclassified -Unlimited<br>Subject Category 31 |

| 19. Security Classif. (of this report) | 20. Security Classif. (of this page) | 21. No. of pages | 22. Price |
|---|---|---|---|
| Unclassified | Unclassified | 92 | A05 |



For sale by the National Technical Information Service, Springfield, VA 22161-2171